Uncertainty assessments of structural loading due to first year ice based on the ISO standard by using Monte-Carlo simulation

Chana Sinsabvarodom [a], Wei Chai [b], Bernt J. Leira [a], Knut V. Høyland [d], Arvid Naess [e]

[a] Department of Marine Technology, Norwegian University of Science and Technology, Norway
[b] Key Laboratory of High Performance Ship Technology (Wuhan University of Technology), Ministry of Education, China
[c] Departments of Naval Architecture, Ocean and Structural Engineering, School of Transportation, Wuhan University of Technology, China
[d] Department of Civil and Environmental Engineering, Norwegian University of Science and Technology, Norway
[e] Department of Mathematical Sciences, Norwegian University of Science and Technology, Norway

A B S T R A C T

Sea ice is the major source of loading for structural design in cold regions. The intrinsic properties of sea ice are generally associated with high degrees of uncertainty due to ice growth taking place during different environ-mental conditions for different areas. The thickness, ice strength coefficient and flexural strength of sea ice are the parameters for the calculation of ice loads. The aim of the present paper is to investigate the uncertainties associated with the ice loads, which are acting on vertical and sloping structures as calculated by the formula-tions in the ISO 19906 standard. The effect of correlation between the key parameters is investigated by using the Nataf transformation model. Monte-Carlo simulation techniques are applied in order to assess the uncertainties associated with the global ice loads due to ice-structure interaction. It is found that for increasing values of the positive correlation between the sea ice properties, the uncertainties of the global ice forces will increase the fractile for both vertical and sloping structures approximately up to 40% and 60% from the case with zero correlation. Moreover, for sloping structures, higher values of the sloping angles imply increasing levels of un-certainty associated with the ice loads.

1. Introduction

The inherent mechanism of ice structure interaction is a complex phenomenon owing to the sea ice properties and interaction process. Structures in the Arctic and Subarctic regions are generally subjected to drifting ice during their time in operation, especially during the winter season. The magnitude of ice loads is typically related to the failure mechanisms of sea ice itself. Different structural configurations imply different failure modes of the sea ice, which are associated with relevant types of ice breaking process. A variety of vertical and sloping structures are typically employed in connection with structural applications such as ships, barges, Gravity-Base Structures (GBS) legs, lighthouses etc. Considering this variety, the characteristics of the sea ice properties are inherently associated with large uncertainties. This implies that repre-sentation of the ice properties and load coefficients as random variables in order to establish a credible probabilistic models is essential. Based on such probabilistic models, structural reliability analysis procedures can be applied in order to quantify the level of safety and integrity of structures in these regions (Bekker et al., 2011b).

During ice-structure interaction, two different and distinct failure mechanisms are observed, which correspond to the flexural versus the crushing failure mode. For vertical structures, the crushing mode is dominating the picture due to confinement of the ice during interaction. However, the loading is significantly reduced when the structural ge-ometry is changed from a vertical to a sloping configuration. This is due to a transition from a crushing to the bending failure mode. Accordingly, this feature can be utilized when performing design of Arctic and Sub-arctic structures in order to obtain more economic structures (Bruun and Gudmestad, 2006).

Inherently, sea ice properties depend on the ice growth conditions related to the climate in a given region. Sea ice samples are typically collected from the target area in order to estimate the sea ice properties by means of field and laboratory tests. The intrinsic properties of sea ice are associated with uncertainties according to the ice features and the

Accepted 8 January 2020

ice conditions (e.g. temperature, salinity, density, porosity, grain size and orientation) (Strub-Klein, 2017).

The design of Arctic and Subarctic offshore structures to withstand the ice loading requires that physical as well as mechanical data of sea ice are available, which can be collected separately. For physical property of sea ice, the ice draft or ice thickness is the main factor, which dominates the ice loading for both vertical and sloping structures. It can be measured by different methods such as satellites, submarines, upward looking sonar (ULS), helicopter-borne electromagnetic instruments (HEM), etc. Different measurement methods provide different accuracy according to the properties of each instrument. For instance, satellites measurements of sea ice can cover a large area but the accuracy is not the best. The HEM can give information about the sea ice thickness only along the flying track of the helicopter. The precision of the HEM method for ice thickness measurement depends on instrumental noise and flying height (Pfaffling et al., 2007). Furthermore, the average daily air temperature from the local measurement stations can be applied with the ice growth model to estimate the level ice thickness in the vicinity area (Li et al., 2016). On the other hand, the mechanical properties of sea ice such as flexural strength, uniaxial strength, ice strength coefficient can only be obtained from experiments or measurements in the field or in the laboratory.

For vertical structures, Zvyagin (2015) introduced an analytical method for the purpose of probabilistic modelling in relation to ice pressure for vertical structures according to the formulation in the ISO standard (ISO, 2010). The thickness and strength coefficient of sea ice were considered as random variables based on the application of a lognormal distribution for both parameters for the purpose of investigating the uncertainty associated with the calculated ice pressure.

For sloping structure, a similar analysis can be performed based on identification of the most important parameters that enter the calculations. It is found that the flexural strength, ice thickness, accumulation of ice rubble and friction coefficients between the sea ice and structures are the dominant quantities for the loading on sloping structures. Ranta et al. (2018) studied the failure of level ice pushing against inclined structures by performing finite discrete element analyses in order to identify the ice failure processes by deterministic and probabilistic methods. The results showed that the ice thickness has a strong effect on the resulting ice load. In the case of deterministic analysis, the initial condition of incoming ice velocity for the simulation model has a significant influence on the ice load estimation. In the probabilistic analysis, it was found that the sample size of the simulated ice data has a significant effect on the accuracy of ice load estimation. The sample size of ice load data for the numerical simulations is relevant for calculation of mean ice load, standard deviation and maximum load as obtained from the time domain simulation.

Ayubian et al. (2016) performed a probabilistic assessment of the ice loading on vertical structures by application of Monte Carlo simulation. The ice thickness and ice strength coefficients of sea ice were treated as the key parameters and were represented by random variables when calculation the exceedance probability for different levels of the ice load. When performing structural reliability analysis, it is important to represent the correlation between the sea ice properties in a proper way due to the strong influence on the resulting loading.

There are several existing national and international standards for determination of the ice loads on offshore structures such as the American API RP 2N (1995), the Canadian CSA S471-04 (2004), the Chinese code Q/HSN 30002002 (2002), the ISO standard (ISO, 19906), the Russian SNiP code 2.06.04.82* (1995) and the Russian VSN code 41.88 (1988) (Thijssen et al., 2014). Frederking (2012) studied the ice pressure on vertical structures resulting from application of different standards (i.e. API, CSA ISO and SNiP). The study was performed based on a deterministic analysis for three different types of structures, i.e. with slender, intermediate and wide loading surfaces. As a result, he recommended that the Canadian CSA-S6-06 (Canadian Highway Bridge Design Code) is suitable for slender and intermediate structures, and the Canadian CSA S471-04 is suitable for wide structures.

For existing offshore structures, Bekker et al. (2011a), studied the global ice loads acting on structures in the OKHOTSK sea for oil and gas fields such as Orlan, Sakhalin-I, Piltun-Astohsky-A&B, Molikpaq, Lunsky-A, and Sakhlin-II. Comparison was made between different national and international design guidelines and Codes. As a result, ice loads based on the SNiP and VSN standards were found to be higher than those computed based on the API, CSA, and ISO standards for a monopile structure. However, for ice loads acting on multi-leg structures, the SNiP and VSN standards provide higher values in comparison with loads from the other Codes.

In order to design offshore structures, all the uncertainties have to be considered. This is required in order to ensure that the structures will be able to perform their intended function with sufficient confidence. The traditional approach in order to deal with uncertainties is to utilize conservative value of the uncertain quantities or safety factors within a deterministic design framework. However, a statistical formulation is also needed owing to the large uncertainties associated with the underlying parameters of the sea ice properties. A reliability-based approach will be of benefit in order to enhance accuracy associated with prediction of extreme events, and also permits to identify proper values of the underlying parameters that define the design values of the ice loading (Wang et al., 2011).

For numerical simulation of ice loading, the discrete element modeling (DEM) approach can be utilized (Tuhkuri and Polojärvi, 2018). There are serval advantages of such a modeling approach. Practically, it can be employed to simulate the ice load on the structures in order to identify the influence of the relevant parameters before performing the physical experiments themselves. Due to the high cost and potential hazard associated with such experiments the numerical studies provides multiple benefits. Moreover, the discrete element modeling approach is widely being used for estimation of design ice loads on the offshore structures. This allows simulation of different design scenarios e.g. in terms of alternative structural configurations and ice conditions. DEM can be applied for simulation of both two and three-dimensional cases, and it allows analysis of both simple and complex ice-structures interaction phenomena. However, only two dimensional solutions has no appropriate defined breaking pattern. For complex structures with irregular geometry such as ship hulls, the discrete element modeling approach has been widely applied for estimation of ice loads (Hisette et al., 2017; Lau et al., 2011). However, this approach requires extensive computer resources, and such simulations are rather time consuming. Typically, upper bound values of the loads are obtained based on extremely severe combinations of the relevant input simulation parameters. Alternatively, repeated simulations with discrete elements models can be performed with different values of the relevant input parameters, which results in significant computational efforts.

The objective of this work is to investigate the uncertainty associated with global ice loads, based on the formulation given in the ISO standard, which has been widely using within the offshore industry. It is emphasized that in the present study, only the statistical scatter of the parameters which are input to calculation of pressure and load are considered, while the model uncertainty associated with the formulation itself is not addressed.

The ice-structure interaction is split into two different scenarios, i.e. vertical versus sloping structures. The effects of correlation between key load parameters are accounted for by application of the Nataf transformation model in order to generate the joint probability distribution based on data obtained from field experiments. Furthermore, the Monte Carlo simulation technique is applied in order to assess the uncertainties associated with the ice pressure and global ice load for the two different scenarios.

2. Environmental condition

2.1. Ice thickness

Ice thickness is the most important parameter when it comes to the resulting magnitude of the global loading on a structure with a given geometry. The present study focuses on first-year sea ice conditions for which the ice thickness conditions are different from multi-year ice. The data related to the maximum annual thickness of level ice is obtained from estimation of air temperature at Rödkallen meteorological station (SHMI, 2019) in northern Gulf of Bothnia Sea. This station can be used to estimate the ice thickness for the Norströmsgrund lighthouse, which is located 23.6 km in north east direction of the station. The observation of the level ice thickness has been measured since 1912. However, a detailed documentation of the measurement sites is not available. Possibly, the measurement sites might have been moved or the environment has changed during the extended observation period (Ronkainen et al., 2018). For the present research, the values of maximum annual level ice thickness from 1952 to 2015 are obtained from Li et al. (2016). From 2016 to 2018, the ice growth model of Zubov (1943), which is the same procedure as applied by Li et al. (2016), is employed in order to estimate the annual maximum values of level ice thickness. The formulation of the ice growth prediction by Zubov model is given in Equation (1).

$$h_i^2 + 50 \cdot h_i = 8 \cdot FDD \tag{1}$$

where h_i denotes the estimated level ice thickness. *FDD* is the accumulated freezing degree days, which is calculated from the daily average temperature, T_d and the freezing temperature of sea water, T_f in the unit of Celsius degree (C^o) as given in Equation (2).

$$FDD = \sum (T_f - \overline{T_d}) \tag{2}$$

It is sufficient to include the daily average temperature below the freezing point of water. The examples of estimation of the level ice thickness by applying the air temperature data obtained from 2000 to 2018 are illustrated in Fig. 1.

The annual maximum of level ice thickness from the calculation of the air temperature by using freezing degree day with Zubov model is validated by comparison with weekly in-situ measurements of the ice thickness by drillings throughout the winter from the Kemi station (Ronkainen et al., 2018), which is located close to the Rödkallen station. The corresponding results are given in Fig. 3.

Fig. 2 shows the annual maximum level ice thickness for 66 years. The mean value and standard deviation of the thickness for the entire data series are equal to 0.66 and 0.17 m respectively. Various probabilistic models are fitted to the level ice thickness data, e.g. the Normal, the Lognormal, the Gamma, the Gumbel and the Weibull distributions. It was found that the normal distribution provides the most appropriate fitting for the level ice thickness as illustrated in Fig. 4. Both the Chi-square and Kolmogorov tests are applied in order to verify the applicability of this distribution at an adequate significance level.

2.2. Ice flexural strength

Typically, sea ice fails in a flexural mode when it interacts with sloping structures. This implies that the flexural strength of sea ice becomes a very important parameter for calculation of the ice loading. This applies in particular to the case of thin ice and slender structures.

The texture of sea ice is dominated by a random alternation between layers with different properties. This inhomogeneous feature of the physical characteristics of sea ice has a significant effect on the stochastic nature of the flexural strength. Flexural testing of sea ice can generally be carried out by three different methods according to the Antarctic Research Institute (AARI) recommendations. These are the cantilever beam tests, three points beam tests and small ice plate tests. Among these tests, the cantilever beam test is the most reliable method because this test is conducted in situ, which allows an assessment of sea ice flexural strength over the whole thickness. Relocation of the sample is also avoided. Disturbance due to relocation can easily generate inaccuracies associated with the test data.

The data set corresponding to flexural strength of sea ice in this study is obtained from Timco and O.'Brien (1994). It is collected during different winter seasons based on different test types, temperature, size of the beam, etc. both in the field and in the laboratory. Data for the flexural strength of sea ice as a function of the root brine volume taken from Timco and O.'Brien (1994) is shown in Fig. 5. The mean value and standard deviation of the sampled data for the flexural strength, are equal to 0.479 and 0.264 MPa, respectively. Different types of probabilistic models have been applied as candidates in order to fit the probability distribution of the flexural strength. It is found that the Weibull distribution given by Eq. (3) provides the most appropriate fit for the present data set. The result of the fitting is shown in Fig. 6 and the scale parameter and shape parameter of the Weibull distribution are determined as 0.5385 and 1.9655 based on regressions coefficients for the straight line fitted in the corresponding probability paper.

$$f(\sigma_f) = \frac{\beta}{\alpha} \cdot \left(\frac{\sigma_f}{\alpha}\right)^{\beta-1} \exp\left(\left(\frac{\sigma_f}{\alpha}\right)^{\beta}\right) \tag{3}$$

2.3. Ice strength coefficient, C_R

The new formulation of the ice-crushing load on the vertical structures with the ISO 19906 standard was developed from the full-scale measurement at the structures. Ice strength coefficients, C_R is

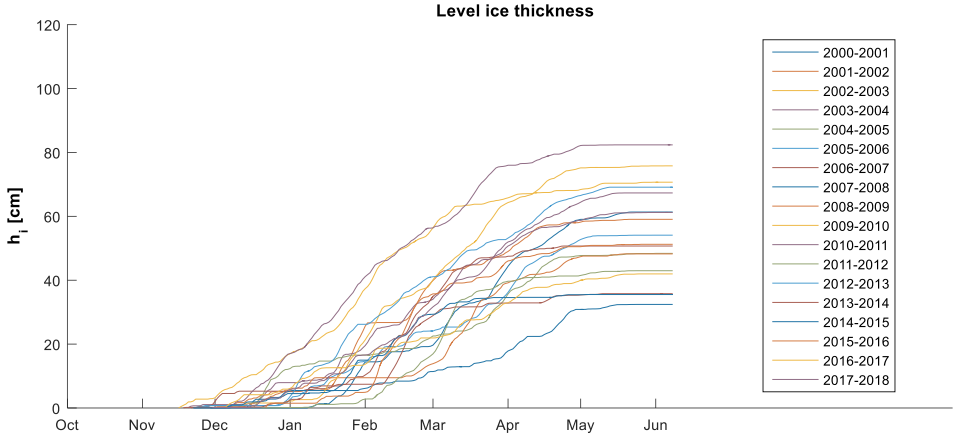

Fig. 1. Estimation of level ice thickness by using air temperature data collected at the Rödkallen meteorological station (Li et al., 2016).

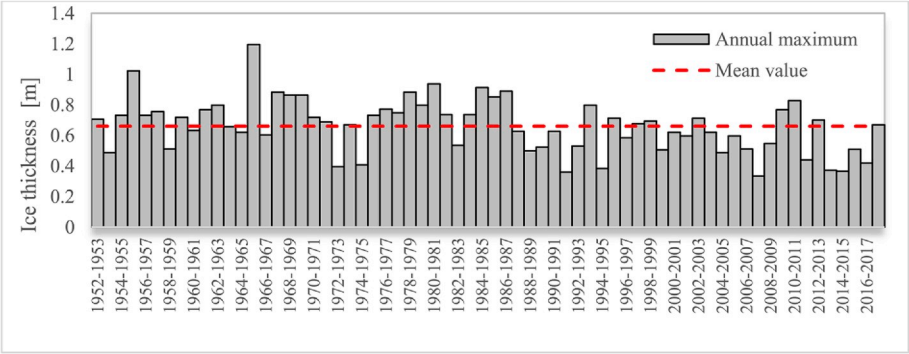

Fig. 2. Estimated maximum ice thickness between 1952 and 2018 (Li et al., 2016).

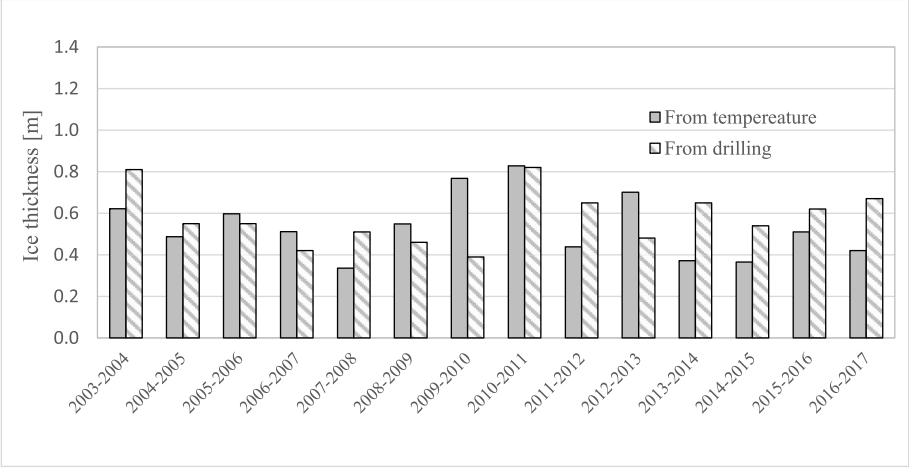

Fig. 3. Comparison of the level ice thickness between drilling measurement and air temperature estimation (Ronkainen et al., 2018).

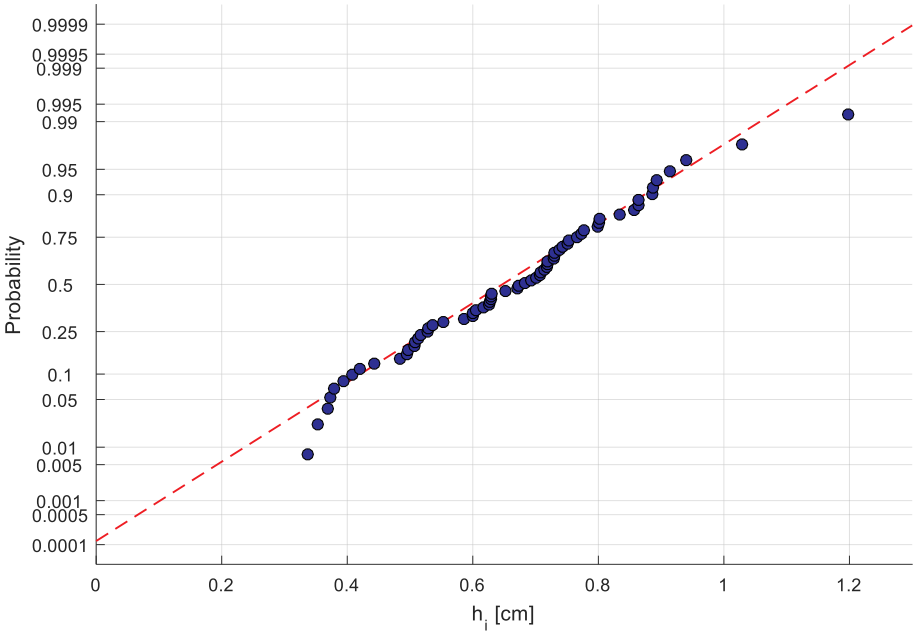

Fig. 4. Fitting the data of the level ice thickness by application of the normal distribution.

introduced as a key parameter in order to estimates ice loading by including the effects of ice-crushing strength, temperature, salinity, etc. into one coefficient (Paquette and Brown, 2017). The value of ice strength coefficient, C_R is depended on the ice properties, which vary corresponding to the climate of the geographical area.

For deterministic analysis, the ISO standard offers the C_R value for alternatives in specific region. The extreme-level ice event (ELIE) is recommended for the ultimate limit state (ULS) design to ensure that no

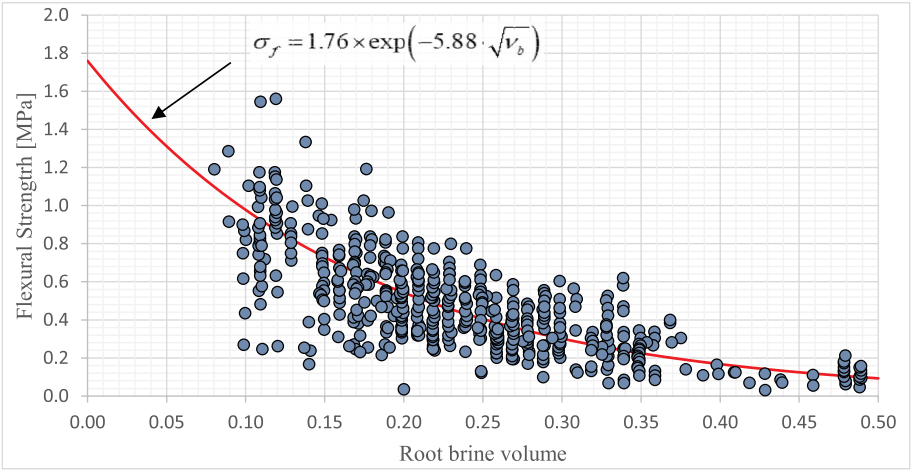

Fig. 5. Flexural strength versus the square root of the brine volume for all test on sea ice (Timco and O.'Brien, 1994).

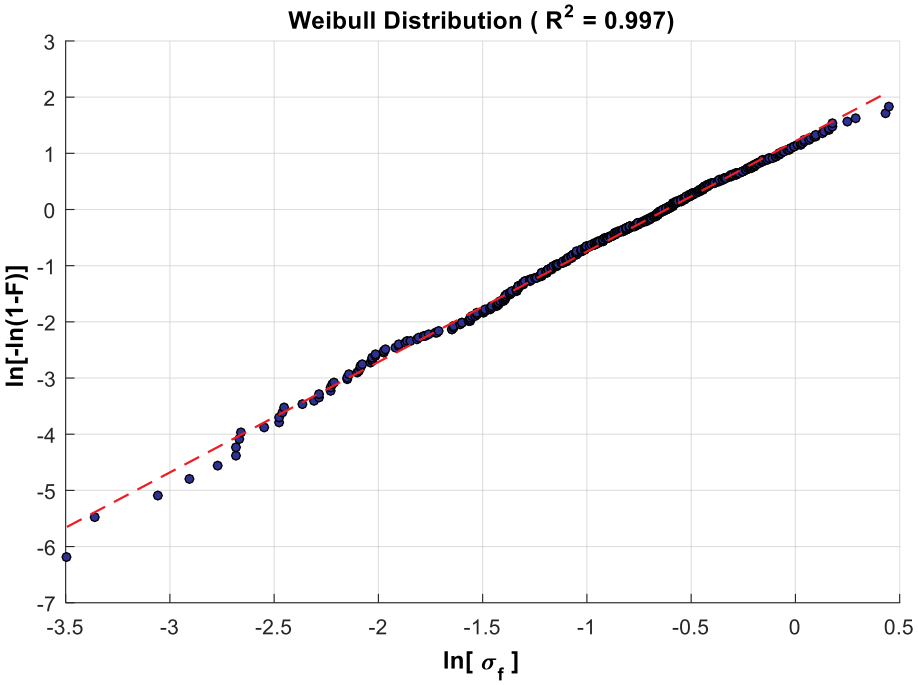

Fig. 6. Fitting the data of flexural strength of sea ice by application of the Weibull distribution.

significant structural damage occurs for both global and local action with an acceptable low probability entire the service life of the structures. The C_R value is originally estimated from the extreme value prediction (Kärnä and Masterson, 2011) with 100-year return period in each specific region with 2.8 MPa for arctic area and 1.8 MPa for a temperature area (ISO, 2010).

This present research use the data of the measured local pressure on lighthouse in Baltic Sea to perform the probabilistic assessment. The data of the strength coefficient C_R is estimated from the maximum peak value of the panel pressures, which were measured at the Norströmsgrund lighthouse from 2000 to 2003 by Kärnä and Masterson (2011) and Kärnä and Yan (2006). The values of ice strength coefficient, C_R are estimated from the backward calculation of the measured ice pressure corresponding to the ISO formulation. The data of ice strength coefficients, C_R with the ice thickness are illustrated in Fig. 8.

Various probabilistic models are fitted to this data. It was found that the Weibull distribution provides the most appropriate fitting as illustrated in Fig. 7. The regression coefficients of the straight line fitting in the corresponding probability paper are applied. These estimators correspond to shape and scale parameter of 4.5044 and 0.4456, respectively. The formula for the probability density function of the Weibull distribution is given in Equation (4), which is of the same type as in Equation (3).

$$f(C_R) = \frac{\beta}{\alpha} \cdot \left(\frac{C_R}{\alpha}\right)^{\beta-1} \exp\left(\left(\frac{C_R}{\alpha}\right)^{\beta}\right) \tag{4}$$

2.4. Correlation between the physical properties of sea ice from experiments

For design of offshore structures with respect to ice loading, the sea ice properties are employed as primary input parameters in order to estimate the ice loading (for a given structural configuration). The magnitudes of the ice loads on the structure are typically strongly dependent on the type of sea ice failure mechanism. There are typically also important effects of the correlation between the ice parameters and

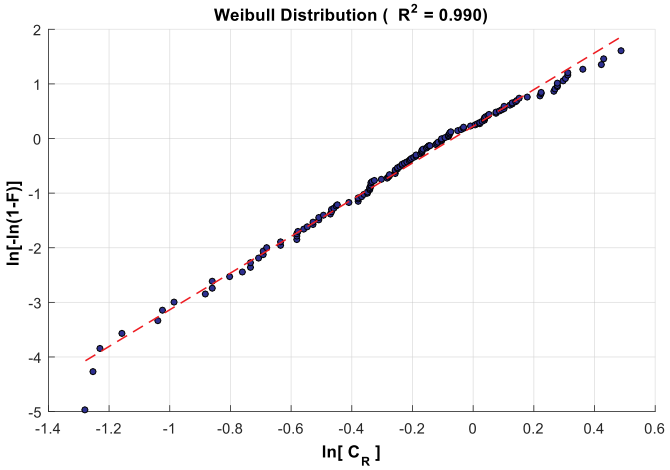

Fig. 7. Fitting the data of ice strength coefficient by application of the Weibull distribution.

the resulting load magnitude. Estimation of these correlation coefficients based on and consideration of underlying physical mechanisms were studied by Leira et al. (2019). Available datasets giving the relationship between the ice properties and the underlying basic variables (e.g. the air temperature) can be utilized for the purposed of quantifying the correlation coefficients between these properties.

For vertical structures, the ice thickness and ice strength coefficient are employed as the key parameters in order to estimate the design ice loading based on ISO (2010). Correlation between the ice thickness and the ice strength coefficient was estimated based on data obtained from load panels attached to the Norströmsgrund lighthouse in the Baltic Sea. The width of the lighthouse at the level of the load panel instruments (which are located at the cold water line (CWL)) is 7.5m. The data points were determined based on ice crushing events corresponding to peak pressures during stationary brittle crushing failure (Kärnä and Masterson, 2011). The degree of correlation between the ice thickness and the ice strength coefficient for different winter seasons during the period from 2000 to 2003 is estimated based on the measurements, which correspond to the points shown in Fig. 8. It is found that the values of correlation coefficients vary between the different winter seasons in the range from −0.41 to 0.41.

For sloping structures, the ice thickness and the flexural strength are in some cases key parameters for estimation of the ice loading (i.e. for relatively thin ice, narrow structures and no snow). This is due to the dominant ice failure mechanism for these cases being the flexural failure mode. In general, the flexural ice strength can be obtain from field experiments. However, field experiments carried out in cold regions have to deal with many kinds of difficulties, such as limited budget, time consuming operations and hard working condition, etc. In particularly, performing flexural testing is very time consuming, which implies that only a few tests can be carried out within a day period. Therefore, the amount of field experimental data related to flexural strength of sea ice is quite limited. For the present research, data of flexural testing from different locations are selected in order to estimate the correlation between the ice thickness and the flexural strength. Estimation of flexural strength was carried out by means of cantilever beam tests. The first and second data sets were digitized from Langhorne and Haskell (2004), who performed flexural testing by means of sea ice cantilever beams and by refreezing cracks of sea ice cantilever beams. For the third and fourth data sets, the flexural testing was conducted around the Svalbard archipelago, i.e. in Svea bay and Lance, respectively, in order to estimate sea ice properties in the north west Barents sea (Ervik, 2013). All experimental data for the flexural testing with different values of the ice thickness are illustrated in Fig. 9.

The values of the correlation coefficient vary between the different data sets within the range from −0.32 to 0.76. The first data set represents conditions with thick level ice. The thickness of the ice specimens varies from 1.79 m to 1.93 m. The air temperature at the ice surface during the experiments was between −15 °C and −21 °C. The correlation coefficient between the ice thickness and flexural strength for this data set has a negative value of −0.310. For second data set, the specimens were refrozen from the first data set in order to perform flexural tests for the same weather condition. The ice thickness of the refrozen specimens at the crack varied from 0.15m to 1.47m. Although the ice thickness of refrozen beams of the second data set is somewhat smaller than for the first data set, the values of the correlation coefficient is −0.322, which is only slightly different from that for the first one. More detailed information in relation to temperature and brine fraction profiles along the level ice thickness are given in Langhorne and Haskell (2004).

For the third data set, the flexural tests of sea ice were performed with six specimens of cantilever beams. These had different lengths and widths, with lengths in the interval 1.5–3.0m and widths in the interval 0.45–0.6m. For the fourth data set, the flexural tests of the cantilever beam specimens were performed with lengths of 7m(3 specimens), 1.5m (1 specimens) and 0.7m(2 specimens), respectively. During the experiments, which were conducted in the North-West Barents Sea, air temperatures at the ice surface varied from about −9 °C to −14 °C (Ervik, 2013). The flexural strength of the sea ice tends to increase with the ice thickness for the present data set. The correlation coefficients for the third and fourth data sets are 0.764 and 0.566, respectively. Merging all the four data sets into one, the estimated value of correlation coefficient between the ice thickness and ice flexural strength is found to be 0.660.

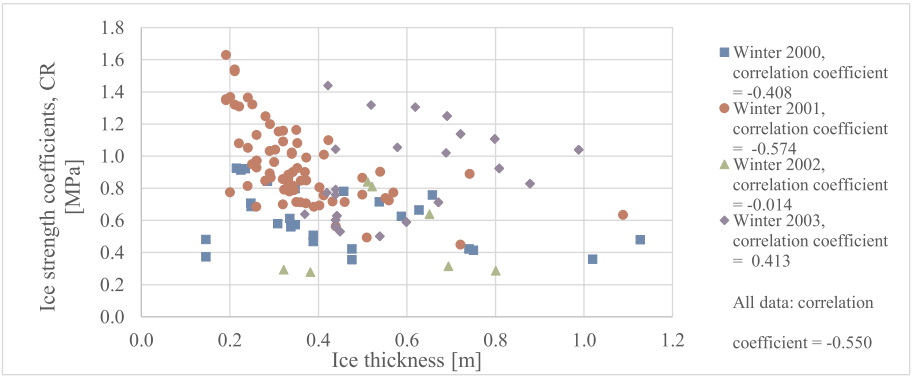

Fig. 8. Joint values of ice thickness and the ice strength coefficient from load panel experiments at the Norströmsgrund lighthouse from 2000 to 2003 (Kärnä and Masterson, 2011).

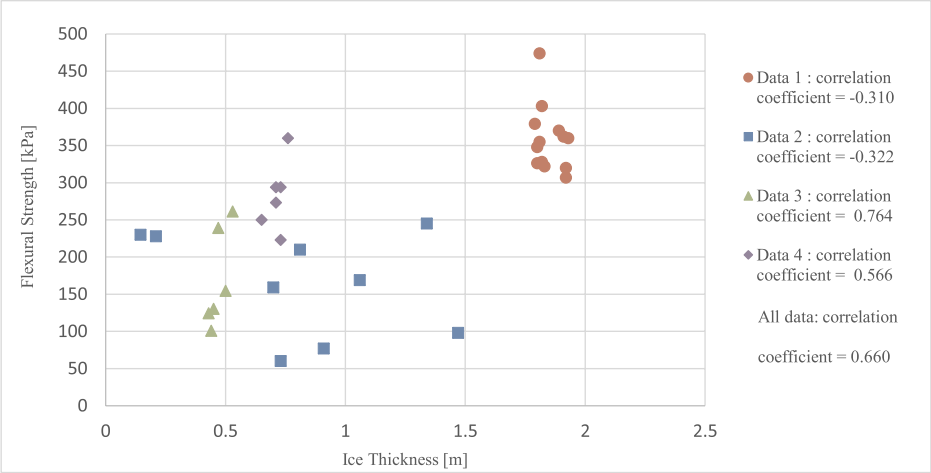

Fig. 9. Joint values of ice thickness and flexural strength of sea ice from field experimental data (Ervik, 2013; Langhorne and Haskell, 2004).

3. Theoretical background

3.1. Probabilistic assessment

The probabilistic assessment procedure in relation to ice structure interaction starts with exploration of the primary ice data associated with the specific site area under consideration, i.e. data corresponding to ice thickness, ice strength coefficient, and flexural strength. Probabilistic models are fitted to the primary ice data. In the present study, the lowest to the highest values of the correlation coefficients are applied in conjunction with the Nataf model. More extensive samples of the random variables are generated for the key parameters by application of MCS techniques. A flowchart illustrating the steps of the probabilistic assessment for ice loading is shown in Fig. 10.

3.1.1. Monte Carlo simulation

Monte-Carlo simulation (MSC) is used to carry out the probabilistic assessment of the loading due to ice structure interaction. In the cases of vertical structures, the samples correspond to different values of the ice thickness and the ice strength coefficient in order to investigate the uncertainty associated with the horizontal ice pressure and global ice loads. In the case of sloping structures, values of the flexural strength of sea ice are generated instead of the ice strength coefficient. The sample values of the level ice thickness x_i, the flexural strength x_j, and the ice strength coefficient x_k are generated from the inverted CDF of the normal distribution, the Weibull distribution, and the Weibull distribution, respectively. The sample values are generated based on random numbers drawn from a uniform distribution, denoted by x_u. The corresponding sample values are given by Equations (5)–(7) below, with the sample size presently being equal to n = 10,000.

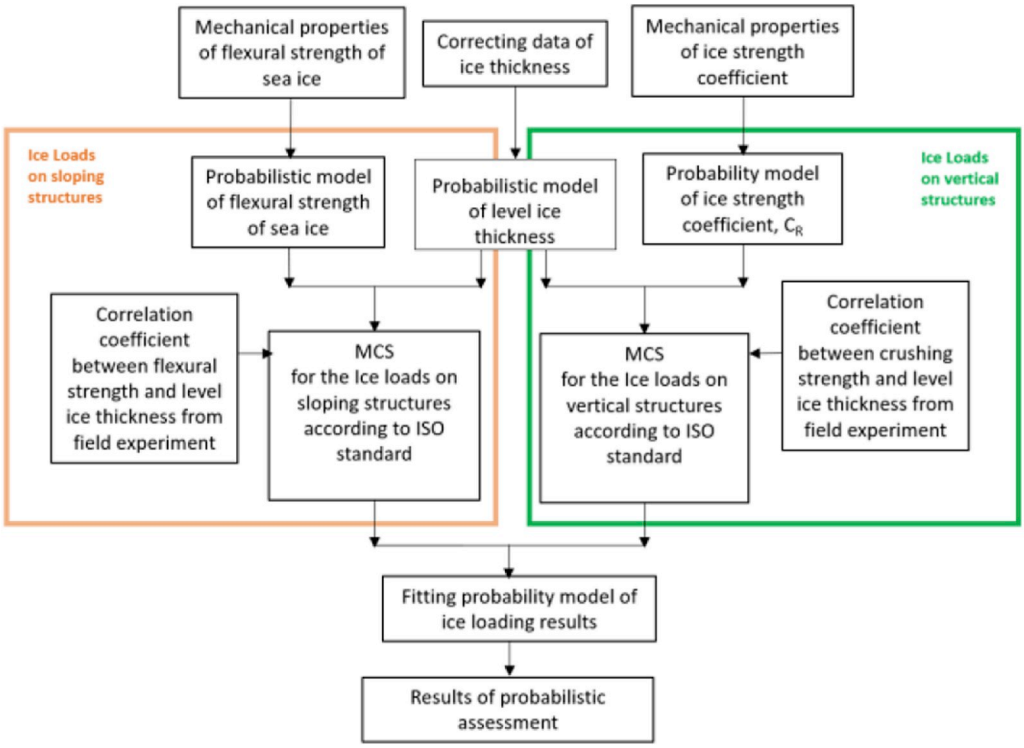

Fig. 10. Flowchart of the various steps entering the probabilistic assessment of ice loads.

For the ice thickness: $x_i = F^{-1}_{thickness}(x_u)$ (5)

For the flexural strength $:x_j = F^{-1}_{flexural}(x_u)$ (6)

For the ice strength coefficient: $x_k = F^{-1}_{crushing}(x_u)$ (7)

The effects of introducing correlation between the key parameters are also investigated in this work. For vertical structures, these parameters are the ice thickness and ice strength coefficient, while for sloping structures these are the ice thickness and the flexural strength.

Independence between the basic variables corresponds to the correlation coefficient ρ being equals to 0, which is first applied as input to the MCS. The scatter diagram with independent ice thickness and flexural strength for sloping structures is shown in the left part of Fig. 11. In the right part, the corresponding scatter diagram for independent ice thickness and ice strength coefficient for vertical structures is shown. Subsequently, the effect of introducing correlation between the variables is studied by application of the NATAF transformation model.

3.1.2. NATAF transformation model

Typically, there will exist correlation between the parameters, which characterize the physical properties of sea ice. This correlation can be estimated based on experimental data. The NATAF transformation model is able to represent this correlation structure in order to generate the corresponding joint probability density and distribution functions (Liu and Der Kiureghian, 1986). The basic assumption behind the NATAF transformation model is that the basic random variables representing the physical properties of sea ice can be obtained by transformation of corresponding Gaussian variables z_i, z_j, z_k and vice versa as given by Equations (8)–(10).

$$z_i = \Phi^{-1}\left(F_{thickness}(x_i)\right) \tag{8}$$

$$z_j = \Phi^{-1}\left(F_{flexural}(x_j)\right) \tag{9}$$

$$z_k = \Phi^{-1}\left(F_{crushing}(x_j)\right) \tag{10}$$

The correlation coefficient $\rho_{0,ij}$ between the two Gaussian variables z_i and z_j is related to the correlation coefficient ρ_{ij} between the thickness x_i and flexural strength of sea ice x_j. The correlation between the random variables representing the physical parameters, i.e. x_i and x_j , is expressed as:

$$\rho_{ij} = \int_{-\infty}^{\infty}\int_{-\infty}^{\infty}\left(\frac{x_i-\mu_i}{\sigma_i}\right)\left(\frac{x_j-\mu_j}{\sigma_j}\right)\phi_2\left(z_i, z_j, \rho_{0,ij}\right)dz_i dz_j \tag{11}$$

where $E(x_r) = \mu_r$, $Var(x_r) = \sigma_r^2$, $r = i, j$ or $r = i, k$; and ϕ_2 is the bivariate standard normal probability density function as given by Equation (12).

$$\phi_2\left(z_i, z_j, \rho_{0,ij}\right) = \frac{1}{2\pi\sqrt{1-\rho_{0,ij}^2}}\exp\left[-\frac{z_i^2 + z_j^2 - 2\cdot\rho_{0,ij}\cdot z_i\cdot z_j}{2\cdot\left(1-\rho_{0,ij}^2\right)}\right] \tag{12}$$

In the Gaussian plane, the uncorrelated variables z_i, z_j can be transformed to correlated variables $\hat{z}_1$ and $\hat{z}_2$ as expressed by Equation (13).

$$\begin{bmatrix}\hat{z}_i \\ \hat{z}_j\end{bmatrix} = \begin{bmatrix}1 & 0 \\ \rho & \sqrt{1-\rho^2}\end{bmatrix}\begin{bmatrix}z_i \\ z_j\end{bmatrix} \tag{13}$$

For vertical structures, the parameter x_k representing the ice strength coefficients in Equations (10) and (12) will be applied instead of the flexural strength of sea ice, i.e. x_j. The NATAF transformation model is valid for the entire range of the correlation coefficient (i.e. between −1 and 1). In the present study, the effect of the correlation between the key parameters of the ice loading acting on vertical and sloping structures is considered. Five values of the correlation coefficient ρ are applied, and these are equal to [-0.9, −0.5, 0.0, 0.5, 0.9]. These cover the relevant range from the smallest to the highest values. The upper and lower values for the correlation coefficient are set as −0.9 and 0.9 due to numerical limitations associated with the transformation (i.e. the transformation matrix in Eq. (13) becomes singular in the limit as the absolute value of the correlation coefficient approaches 1.0). The corresponding scatter diagrams based on application of the Nataf transformation model for different values of the correlation coefficient to perform the uncertain assessment of ice loading on vertical and sloping structures are demonstrated in Figs. 12 and 13, respectively.

3.2. Ice interaction with structures

3.2.1. Ice load on vertical structures

For vertical structures, the mechanism of ice failure typically corresponds to the crushing mode. The formulation of the ice pressure p_G based on the ISO 19906 standard is given in Equation (14).

$$p_G = C_R\left(\frac{h}{h_1}\right)^n\left(\frac{w}{h}\right)^m \tag{14}$$

where C_R is the ice strength coefficient, h is the ice thickness, h_1 is a reference thickness of 1 m, w is the width of the structure, m is an empirical coefficient equal to −0.16, n is an empirical coefficient equal to $(-0.5 + h/5)$ for $h < 1.0$ m and equal to −0.30 for $h \geq 1.0$ m (ISO, 2010).

For ice crushing against a vertical structure, the global ice load, F_G occurs perpendicular to the contact surface according to the limit

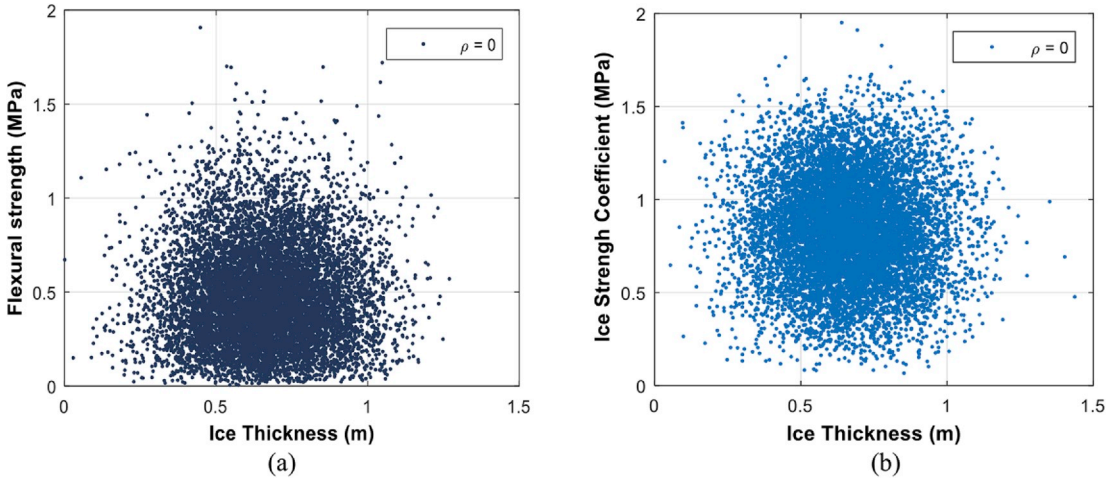

Fig. 11. Illustration of independent samples based on MCS a) ice thickness and flexural strength and b) ice thickness and ice strength coefficient.

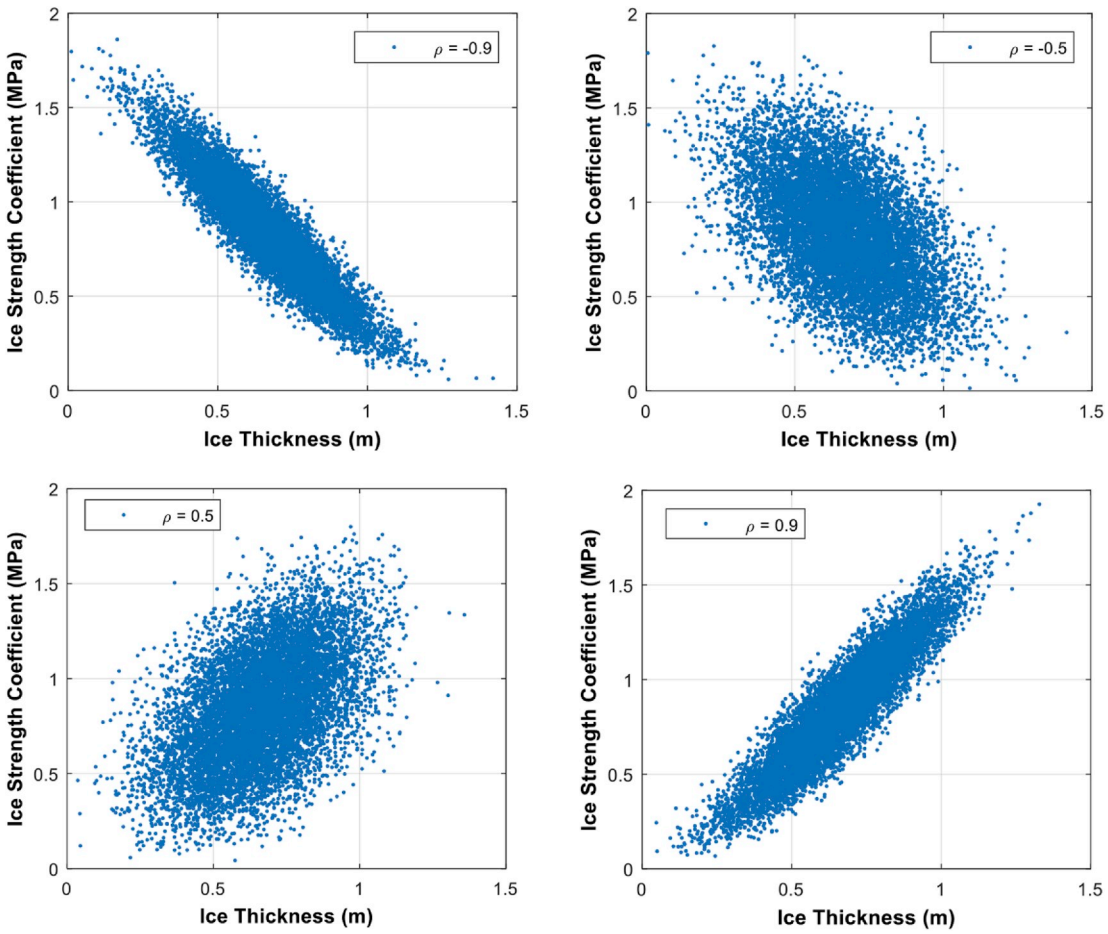

Fig. 12. Samples based on the joint probability distribution function of ice strength coefficient and ice thickness for the vertical structures by application of the NATAF transformation model with the correlation coefficients.

mechanism of ice failure and is expressed in terms of Equation (15).

$$F_G = p_G \cdot h \cdot w \tag{15}$$

In the present study, different structural widths are considered, i.e. 1 m, 4m, and 10m. This is in order to investigate the resulting influence of the width on the computed ice pressure and the global ice force in connection with the probabilistic assessment based on application of Monte-Carlo simulation.

3.2.2. *Ice load on sloping structures*

In the present study focus is on ice loading calculated according to the formula suggested by the ISO 19906 standard, which is based on the theory of beam bending on an elastic foundation (Croasdale and Cammaert, 1994; ISO, 2010). Inclined slope configurations can be divided into two main categories, which correspond to upward and downward slopes as illustrated in Figs. 14 and 15, respectively.

In the case of downward sloping structures, the weight of the ice fragments or ice rubbles due to fracture of ice sheet will be considered as a submerged weight, which takes into account the effect of buoyancy.

The major components of the global ice loads can be decomposed into the horizontal and vertical directions. These components are functions of normal component (N) of ice action on the structure, the sloping angle (α) and the friction coefficient (μ_{st}) of the surface roughness between sea ice and the structure. The formula of horizontal ice force (F_H) and vertical ice force (F_V) can be expressed by Equations (16) and (17).

$$F_H = N \sin\alpha + \mu_{st} N \cos\alpha \tag{16}$$

$$F_V = N \cos\alpha - \mu_{st} N \sin\alpha \tag{17}$$

The loading ratio (ξ) calculated from the horizontal and vertical ice load components is expressed by Equation (18).

$$\xi = \frac{F_H}{F_V} = \frac{\sin\alpha + \mu\cos\alpha}{\cos\alpha - \mu\sin\alpha} \tag{18}$$

In the ISO 19906 standard, the horizontal global ice load is subdivided into five components according to the interaction mechanism. These are as follows: The breaking load (H_B), the load component required to push the sheet ice through the ice rubble (H_P), the load required in order to push the ice blocks up the slope through the ice rubble (H_R), the load required to lift the ice rubble on top of the advancing ice sheet prior to breaking it (H_L)and the load needed to turn the ice block at the top of the slope (H_T). This formulation is expressed by means of Equation (19).

$$F_H = \frac{H_B + H_P + H_R + H_L + H_T}{1 - \frac{H_B}{\sigma_f \cdot l_c \cdot h}} \tag{19}$$

where, l_c is the total length of the circumferential crack. The breaking load component (H_B) is the major loading, which corresponds to bending of ice sheet, which invokes the flexural strength, σ_f of the sea ice and results in the following expression:

$$H_B = 0.68 \cdot \xi \cdot \sigma_f \left(\frac{\rho_w \cdot g \cdot h^5}{E}\right)^{0.25} \cdot \left(w + \frac{\pi^2 \cdot L_c}{4}\right) \tag{20}$$

where, ρ_w is the density of seawater, g is gravitational acceleration, w is

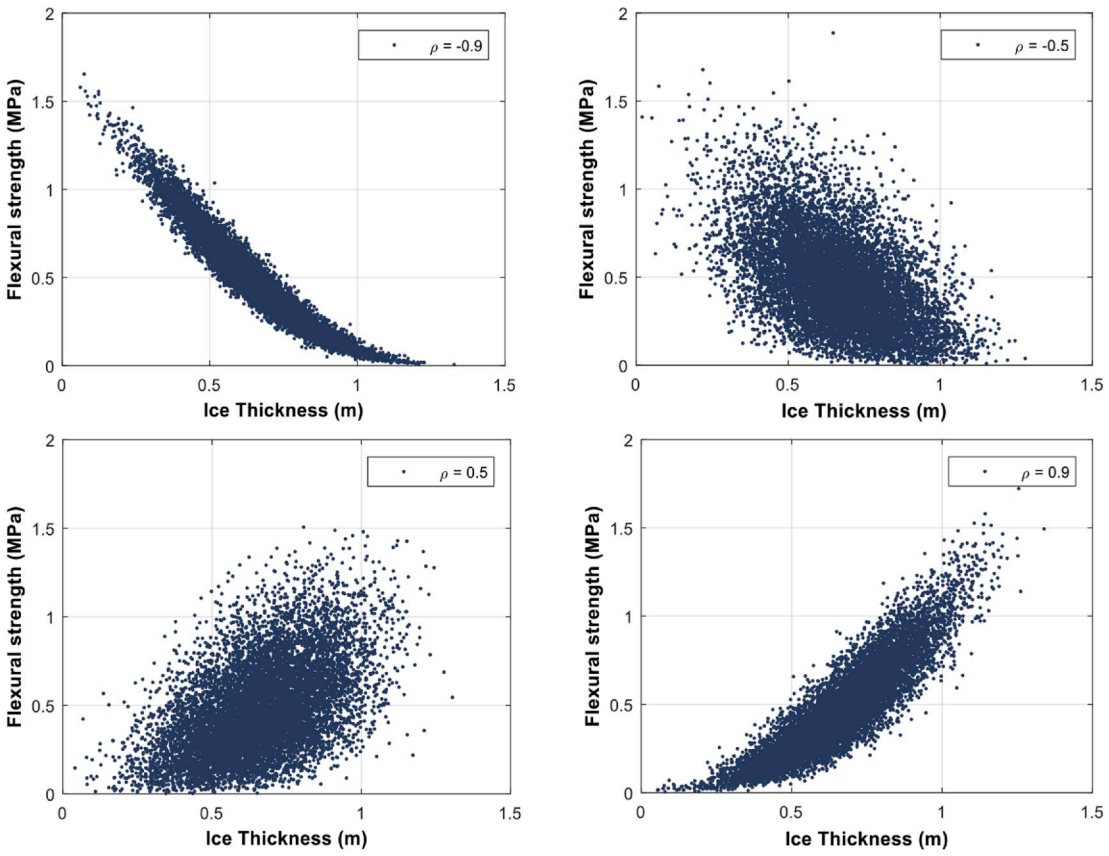

Fig. 13. Samples based on the joint probability distribution function of flexural strength and ice thickness for the sloping structures by application of the NATAF transformation model with the correlation coefficients.

the width of the structure. During the ice-structure interaction, the length of the ice sheet between the interaction domain and the location of the fracture position is referred to as the critical length (L_c). The theoretical formulation for the critical length is based on elastic plate bending as given by Equation (21):

$$L_c = \left[\frac{E \cdot h^3}{12 \cdot \rho_w \cdot g \cdot (1 - \upsilon^2)}\right]^{1/4} \tag{21}$$

where E and υ is the elastic modulus and the Poisson ratio, respectively.

In order to push the advancing ice sheet through the ice rubble, the load component H_P arises, which is given as:

$$H_P = w \cdot h_r^2 \cdot \mu_i \cdot \rho_i \cdot g \cdot (1 - e) \cdot \left(1 - \frac{\tan\theta}{\tan\alpha}\right)^2 \frac{1}{2\tan\theta} \tag{22}$$

Where h_r is the rubble height, μ_i is the friction coefficient of ice-to-ice rubble, ρ_i is the density of the sea ice, $e$is the porosity of the ice rubble, θ is the angle the rubble makes with the horizontal plane.

The additional force required in order to push the ice blocks up the slope through the ice rubble is the load component H_R as given by Equation (23):

$$H_R = w \cdot P \frac{1}{\cos\alpha - \mu_{st}\sin\alpha} \tag{23}$$

The parameter P is expressed by Equation (24).

$$P = 0.5 \cdot \mu_i(\mu_i + \mu_{st}) \cdot \rho_i \cdot g \cdot (1 - e) \cdot h_r^2 \cdot \sin\alpha \cdot \left(\frac{1}{\tan\theta} - \frac{1}{\tan\alpha}\right) \cdot \left(1 - \frac{\tan\theta}{\tan\alpha}\right) + \ldots$$
$$\ldots + 0.5(\mu_i + \mu_{st}) \cdot \rho_i \cdot g \cdot (1 - e) \cdot h_r^2 \cdot \frac{\cos\alpha}{\tan\alpha} \cdot \left(1 - \frac{\tan\theta}{\tan\alpha}\right) + h_r \cdot h \cdot \rho_i \cdot g \cdot \frac{\sin\alpha + \mu_{st}\cos\alpha}{\sin\alpha} \tag{24}$$

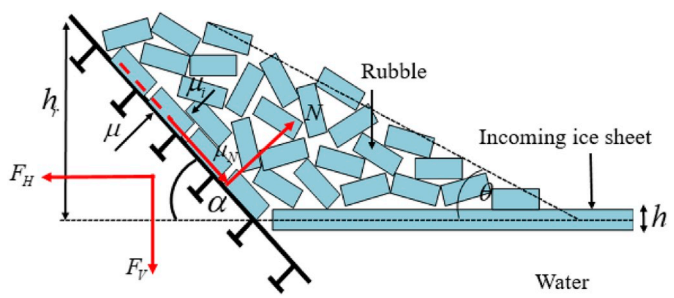

Fig. 14. Ice-structure interaction with upward slope.

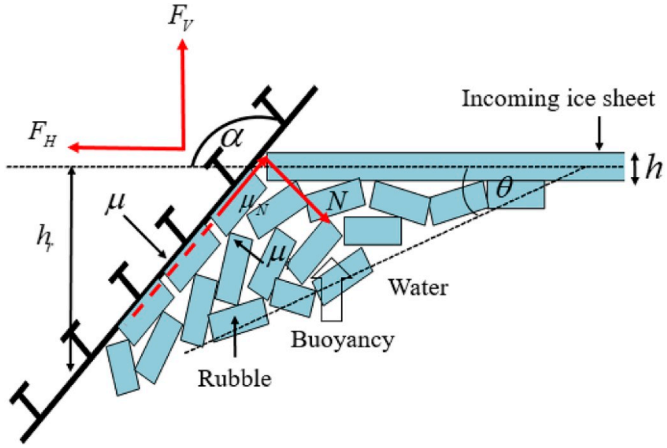

Fig. 15. Ice-structure interaction for the case of a downward slope.

The load component H_L is given in Equation (25):

$$H_L = 0.5 \cdot w \cdot h_r^2 \cdot \rho_i \cdot g(1-e) \cdot \xi \cdot \left(\frac{1}{\tan\theta} - \frac{1}{\tan\alpha}\right) \cdot \left(1 - \frac{\tan\theta}{\tan\alpha}\right) + \ldots$$
$$\ldots + 0.5 \cdot w \cdot h_r^2 \cdot \rho_i \cdot g(1-e) \cdot \xi \cdot \tan\varphi \cdot \left(1 - \frac{\tan\theta}{\tan\alpha}\right)^2 + \xi \cdot c \cdot w \cdot h_r \cdot \left(1 - \frac{\tan\theta}{\tan\alpha}\right) \quad (25)$$

where c is the cohesion of the ice rubble and φ is the corresponding friction angle.

The load component H_T is due to turning of the ice block at the top of the slope as given by Equation (26):

$$H_T = 1.5 \cdot w \cdot h^2 \cdot \rho_i \cdot g \frac{\cos\alpha}{\sin\alpha - \mu_{si}\cos\alpha} \quad (26)$$

During the interaction between the ice and the sloping structure, the extent of ride up of the rubble pile is significantly enlarged due to accumulation of ice fragments. Empirical formulas obtained from data collected at the Kemi-I lighthouse and the Confederation bridge are applied in order to calculate the rubble pile height (Brown and Määttänen, 2009). The heights of ice ride-up or rubble pile-up are related to the water level or the level ice surface. For the Kemi-I lighthouse, the rubble pile-up height increases linearly as illustrated in Equation (27). For the Confederation bridge, the rubble pile-up increases according to a power law function as given in Equation (28).

$$h_r = 3 + 4 \cdot h \quad (27)$$

$$h_r = 7.64 \cdot h^{0.64} \quad (28)$$

The relationship between rubble pile-up height versus level ice thickness are illustrated in Fig. 16.

The rubble pile-up height is a function of the level ice thickness. The PDF of the rubble pile-up height can be calculated by using a one-to-one transformation for the monotonously increasing function, which is given in Equation (29). Two different rubble pile-up height PDFs are plotted in Fig. 16 for two different cases (i.e. the Kemi-I light house and the Confederation bridge). In this analysis, the Confederation bridge formula is applied to calculate the rubble pile-up height because it provides higher value from the estimation, which can be observed from the PDFs in Fig. 16. Therefore, more conservative global forces would be estimated

$$f_{h_r}(h_r) = f_{h_i}\left(h = g^{-1}(h_r)\right)\frac{dh}{dh_r} \quad (29)$$

where $g(.)$ is the functional relationship of rubble pile-up height in the relevant area of level ice thickness as illustrated in Fig. 17.

The sea ice will get in contact with the surface area of the structures during the interaction. The friction coefficient is therefore important to estimate the global ice loading. The value of the friction coefficient between the sea ice and the structure (Saeki et al., 1986) depends on the temperature, contact speed, and surface roughness. The value of the friction coefficient for the present analysis is based on the average value of ice drift speed in the Barents Sea as given in Table 1.

The input parameters for investigation of the uncertainty associate with the global ice load on sloping structures, (i.e. upwards or downwards), based on formulation of ISO 19906:2010, are presented in Table 1.

In addition, the analysis considers ice breaking in both the upward and downward directions. Each slope category is divided into three different angles as listed in Table 2.

4. Results

According to the ice loads on structures obtained by application of the ISO standard, the analysis of ice load is different for vertical versus sloping structures. Basically, this is due to the sea ice failure mechanisms being different for the two cases which correspond to the crushing mode and the flexural mode, respectively.

4.1. Vertical structures

In the first part below, results for the average ice pressure and the global ice loads on vertical structures are presented. The ice pressure is found to be a decrease function when the structural width and ice thickness increase due to the scaling effect. Interestingly, the values of the ice pressure increase dramatically when the ice thickness is lower than 0.25 m as illustrated in Figs. 18 and 19 (a). This is because of the power term of aspect ratio from ISO formulation in Equation (14). Furthermore, the global ice forces on the vertical structures demonstrates an increasing function with the ice thickness, the width of the structure, and the ice strength coefficient as illustrated in Fig. 19 (b). The results imply that the range of thin ice thickness provides the higher ice pressure on the local members of the structures, which may leads to higher local member stresses. Moreover, the average ice pressure of ISO formulation does not take into account the effect of the imperfection of the contract area in the high pressure zone or critical zone, which can promote the higher local ice pressure due to the confinement during of the ice-structure interactions process. Nevertheless, Jordaan (2001) found that the high-pressure zone of the contact area in case of thin ice is

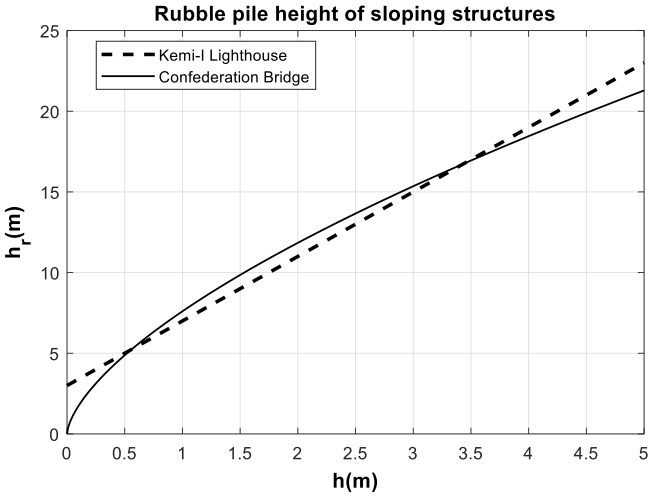

Fig. 16. The relationship between level ice thickness and rubble pile height.

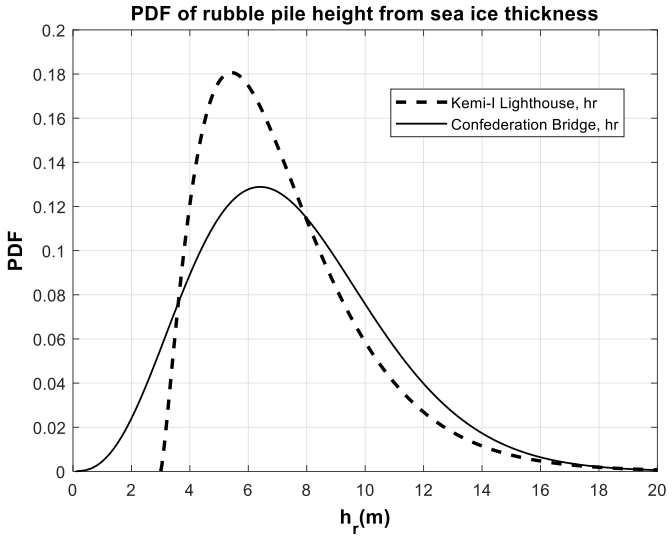

Fig. 17. Probability density functions of the rubble pile height.

Table 1
The input parameters for calculation of ice loads on sloping structures.

Data	Value
Elastic Modulus of ice, E_i	567.46 kPa
Ice density, ρ_i	977 kg/m^3
Water density, ρ_w	1025 kg/m^3
Ice Poisson Ratio, ν	0.3
The water line diameter, w	1.0 m
The cohesion of the ice rubble, c	5 kPa
The porosity of the ice, e	0.2
The angle of internal friction, φ	40 deg.
The coefficient of friction between the ice and the structures, μ	0.07
The coefficient of friction between pieces of ice, μ_i	0.01

Table 2
Variation of slope angles for ice structure interaction.

Up slope (deg.)	Down slope (deg.)
30	120
45	135
60	150

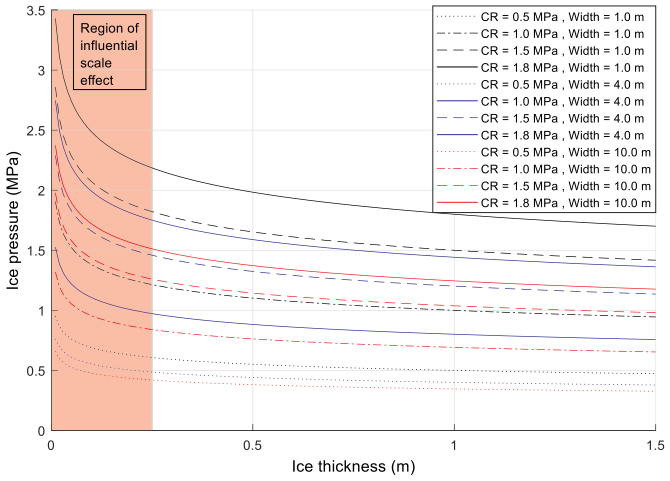

Fig. 18. The influence of scale effect for the ice pressure on the vertical structure.

not significant for local ice pressure.

As part of the probabilistic assessment, the effects of correlation between the ice thickness and the ice strength coefficient in connection with ice pressures and global ice forces based on the NATAF transformation model are investigated. Numerical samples based on the NATAF transformation model for a correlation coefficient equal to −0.5 in the planes of average ice pressure and global ice force are shown in Fig. 20. It can be seen that some data points from the numerical samples are located in the region where scale effects are important. Higher negative values of the correlation coefficients between the ice thickness and the ice strength coefficient tend to generate more sample data points in the region where scale effects are of significance. However, those sample points do not correspond to high values of the global ice force.

The statistical parameters based on the MCS results for vertical structures are given in Table 3 in terms of mean value, standard deviation, and coefficient of variation (COV) of the ice pressure per square metre and global ice load. The COV indicates the degree of dispersion of the probability distribution of the ice loads. Slender structures (i.e. with small width) tend to exhibit higher mean values of the ice pressure per square metre than wider structures owing to the scale effect of sea ice. The lower correlation between ice thickness and ice strength coefficient demonstrates higher uncertainty for average ice pressures, which can be observed from the higher values of COV and standard deviation. On the contrary, the uncertainty in the global ice forces demonstrates the opposite trends, which values of standard and COVs increase according to the effect of correlation between ice thickness and ice strength coefficient.

The results of the ice pressure and global ice loading are presented in the box-and-whisker diagram to illustrate the data distribution in the connection with the interquartile range (IQR). The IQR is defined from the 25th percentile, Q_1 and the 75th percentile, Q_3 as IQR = Q_3-Q_1. The middle line inside each of the rectangular boxes demonstrates the median and whiskers above and below the box demonstrates the location of the minimum and maximum of 1.5 IQR. Lower values of the correlation coefficient between the ice thickness and the ice strength coefficient for average ice pressure implies a high level of dispersion, which also means that a larger number of data points will exceed the maximum whisker limits as illustrated in Fig. 21. On the contrary, the results for the global ice forces exhibit an opposite trend as illustrated in Fig. 22. For each box-and-whisker diagram of the ice pressure and the ice force, the central mark indicates the median, and the bottom and top edges of the box indicate Q_1 (25th percentiles) and Q_3 (75th percentiles), respectively. The bottom and top whiskers limits indicate $Q_1 - 1.5 \times$ IQR and $Q_3 + 1.5 \times$ IQR, respectively (https://ch.mathworks.com/help/stats/boxplot.html).

The samples obtained based on the Monte Carlo simulation are applied for the purpose of distribution fitting. This allows us to investigate the statistical characteristic of the global ice loads for vertical structures. An example of a quality plot for fitting the average ice pressure and global ice forces acting on vertical structure (for a correlation coefficient, $\rho = 0.5$ and a width of 1.00 m) by application of the Weibull distribution is illustrated in Fig. 23.

The correlation coefficient has a significant effect on the shape of the probability density function of the average ice pressure and global ice forces. The flat shape of PDF implies the higher dispersion or uncertainty, which contains inside the random variables. The average ice pressure trends to have flatter shape when the value of correlation coefficients between ice thickness and ice strength coefficient decrease. Whereas, the opposite trend between the average ice pressure and global ice forces also addresses on the PDFs. The Weibull probability density functions (PDF) of ice pressures and global ice loading are displayed in Fig. 24.

The effect of varying correlation on the average ice pressure can also be studied by comparison of the respective cumulative density functions (CDF) for different values of the correlation coefficients. These are shown the same trends with PDFs as illustrated in Fig. 25 in which the effect of structural width is also illustrated.

4.2. Sloping structures

For sloping structures, the global ice loads from the ISO formulation increase significantly with increasingly steeper slopes in both the upward and downward slope directions. The magnitude for the global ice loads in the horizontal direction are higher than those in the vertical direction, and the values of ice load in the horizontal direction is more sensitive to the sloping angles than vertical direction, which can be observed in Fig. 26.

For Monte Carlo simulation, the samples of vertical and horizontal ice loads are generated from the basic variables of ice thickness and flexural strength, based on the ISO formulation. After that, the application of NATAF transformation model is applied to simulate the dependency between the basic variables corresponding to the correlation coefficient,ρ. The examples of scatter diagrams for horizontal and vertical loads with dependent correlation coefficient between ice thickness and flexural strength for upward and downward slopes directions are shown in Figs. 27 and 28, respectively.

The statistical parameters of the horizontal and vertical ice loads on

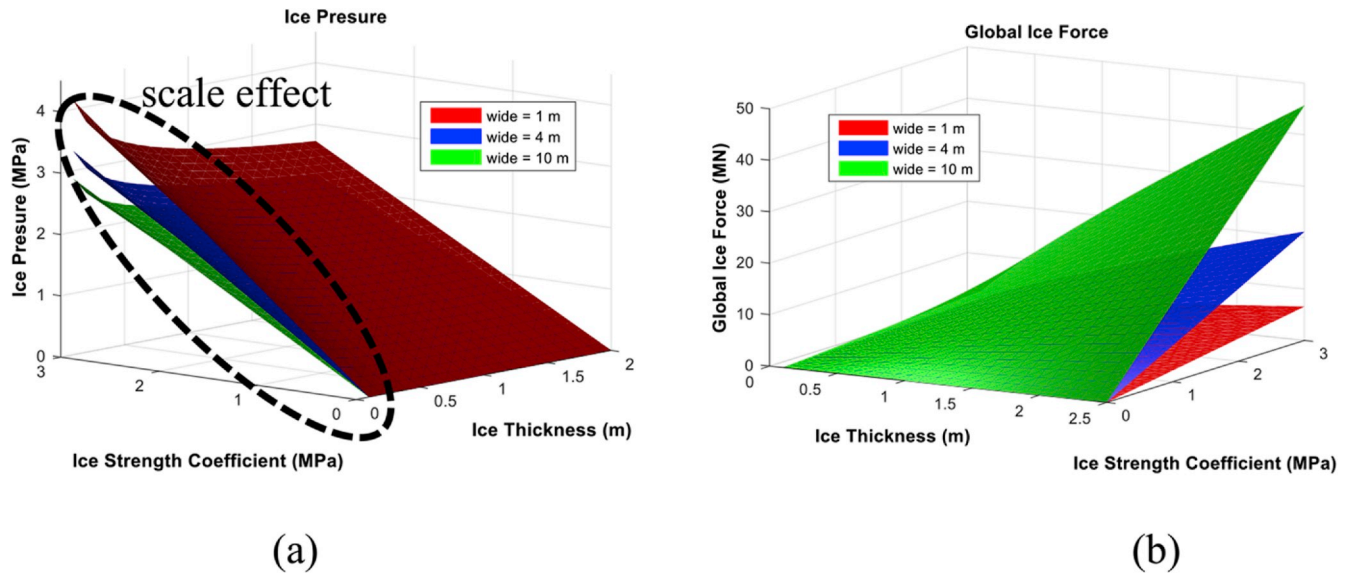

Fig. 19. a) Relationships of the average ice pressure and global ice loads as functions of ice thickness and ice strength coefficient for varying structural widths.

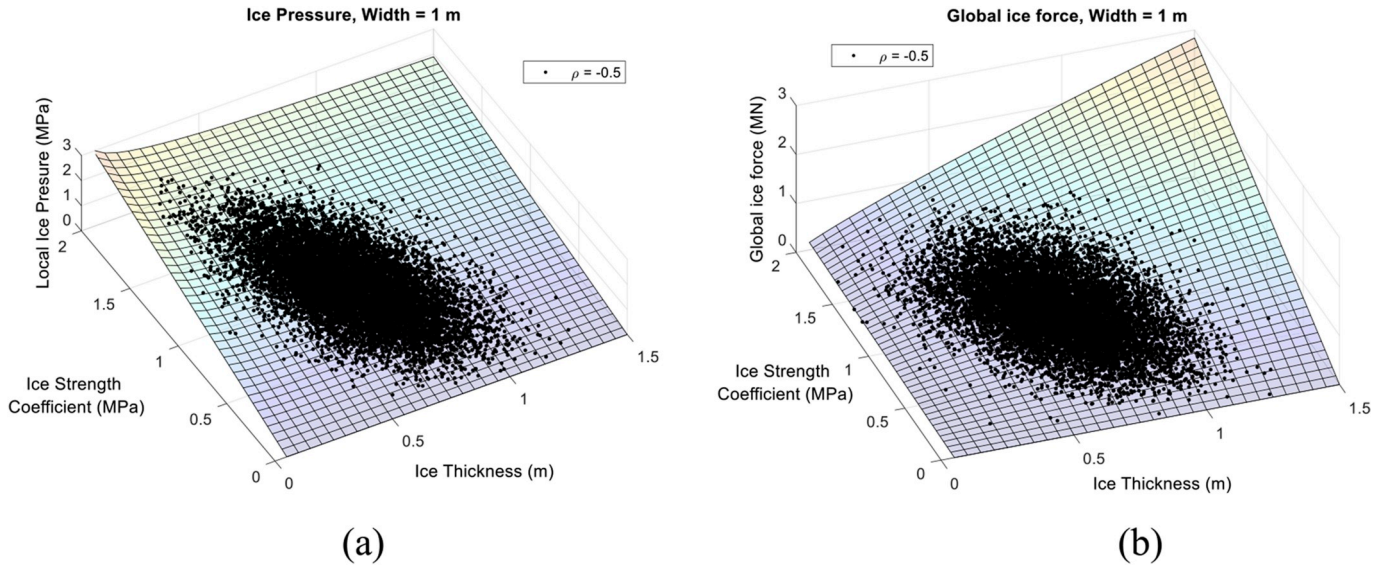

Fig. 20. Samples of the average ice pressures and global ice forces based on an application of the NATAF transformation model for $\rho = 0.5$ and w = 1 m.

Table 3
Statistical characteristics of ice pressure and global ice load of vertical structures for different structural widths.

Width (m)	ρ	Ice pressure (MPa)				Global ice force (MN)			
		Mean	STD	COV %	Kurtosis	Mean	STD	COV %	Kurtosis
1	−0.9	0.96	0.42	43.58	7.06	0.57	0.12	20.60	3.74
1	−0.5	0.95	0.38	40.19	4.40	0.59	0.18	31.34	3.06
1	0.0	0.94	0.33	35.34	3.51	0.61	0.24	39.97	3.13
1	0.5	0.93	0.29	31.21	3.50	0.63	0.29	45.70	3.28
1	0.9	0.91	0.26	28.35	2.71	0.65	0.33	50.43	3.61
4	−0.9	0.77	0.33	43.09	7.28	1.82	0.38	20.75	3.95
4	−0.5	0.76	0.30	39.10	4.10	1.88	0.59	31.26	3.00
4	0.0	0.75	0.27	35.53	3.46	1.94	0.77	39.68	3.18
4	0.5	0.74	0.23	31.39	2.78	2.02	0.94	46.45	3.50
4	0.9	0.73	0.21	28.61	2.77	2.06	1.05	51.09	3.57
10	−0.9	0.66	0.29	43.77	5.45	3.92	0.80	20.38	3.72
10	−0.5	0.66	0.26	39.69	4.19	4.05	1.25	30.88	3.02
10	0.0	0.65	0.23	34.97	3.28	4.19	1.69	40.27	3.09
10	0.5	0.64	0.20	31.28	2.75	4.39	2.04	46.45	3.36
10	0.9	0.63	0.18	28.25	2.76	4.48	2.27	50.74	3.69

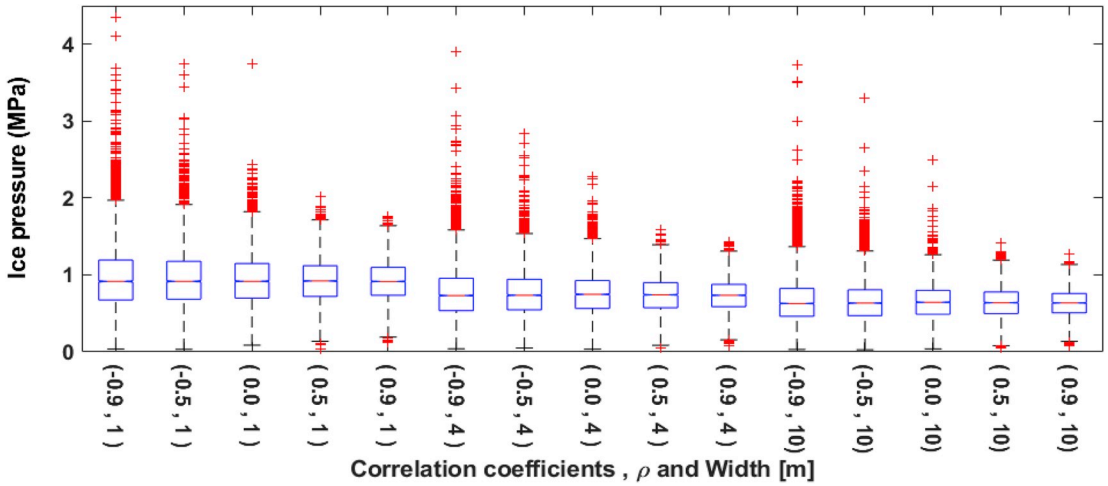

Fig. 21. Box-and-whisker diagram for average ice pressures on vertical structure with different correlation coefficient and different structural widths.

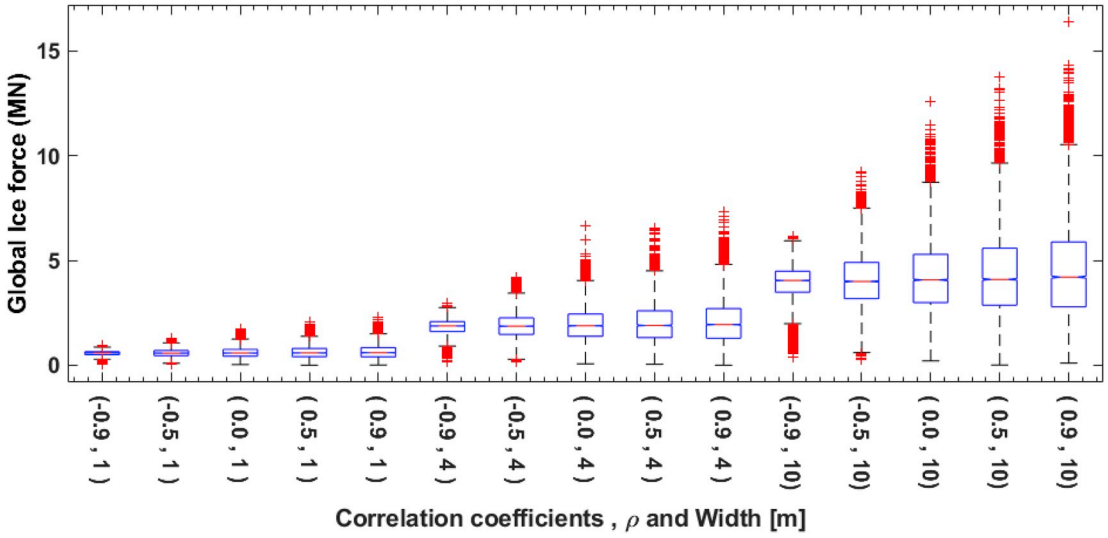

Fig. 22. Box-and-whisker diagram for global ice forces on vertical structure with different correlation coefficient and different structural widths.

sloping structures in upward and downward direction given in terms of mean values, standard deviations, COVs, and Kurtosis are listed in Tables 4 and 5, respectively. The results for the ice loads on sloping structure can be indicated the level of uncertainties by using statistical parameter with coefficient of variation (COV).

For global horizontal ice load, steeper slope geometries provide higher loading magnitudes and higher uncertainties. The values of the COV are increasing with steeper slopes and higher value of correlation coefficients between ice thickness and flexural strength. The breaking load component H_B is the major loading, which corresponds to the bending of the ice sheet to invoke the flexural failure of the sea ice.

The global vertical ice loads on the sloping structures are also demonstrated the same pattern with the horizontal ice loads, however the mean values of ice loading do not change so much with varying sloping angles. Higher correlation between the ice thickness and flexural strength leads to higher dispersion of PDFs, which corresponds to higher statistical uncertainty. The value of the COV demonstrates an increasing function of the correlation coefficient for both upward and downward sloping structures.

The results of horizontal and vertical ice forces on the sloping structure are demonstrated in the box-and-whisker diagram to present the data in the interquartile range (IQR). For horizontal ice force, the higher correlation coefficients between ice thickness and flexural strength provide higher uncertainty, which can be observed from the longer length of box spans and whisker length as illustrated in Fig. 29. Whereas, the vertical ice forces present almost the same trend of data distributions with horizontal ice forces when changing slop angles. The uncertainty related to vertical ice forces are mainly dependent on the correlation coefficients between ice thickness and flexural strength. However, the median of the vertical ice force does not vary much in comparison with the horizontal ice forces as shown in Fig. 30. For each box-and-whisker diagram for the horizontal and the vertical ice forces, the central mark indicates the median, and the bottom and top edges of the box indicate Q_1 (25th percentiles) and Q_3 (75th percentiles), respectively. The bottom and top whisker limits indicate $Q_1 - 1.5 \times \text{IQR}$ and $Q_3 + 1.5 \times \text{IQR}$, respectively.

Various types of probabilistic models have been applied as the candidates to fit the distributive results of horizontal and vertical ice forces. As a result, the Weibull distribution provide the most appropriate fit for the component of global ice force on the sloping structures. The example of the PDF fitting with horizontal and vertical ice force by the Weibull distribution is illustrated in Fig. 31.

Flatter slopes provide significantly reduction for the loading magnitude in horizontal direction owning to the transformation of failure mechanism of sea ice from crushing mode to bending mode. The uncertainty of global ice loads on sloping structure in upward and

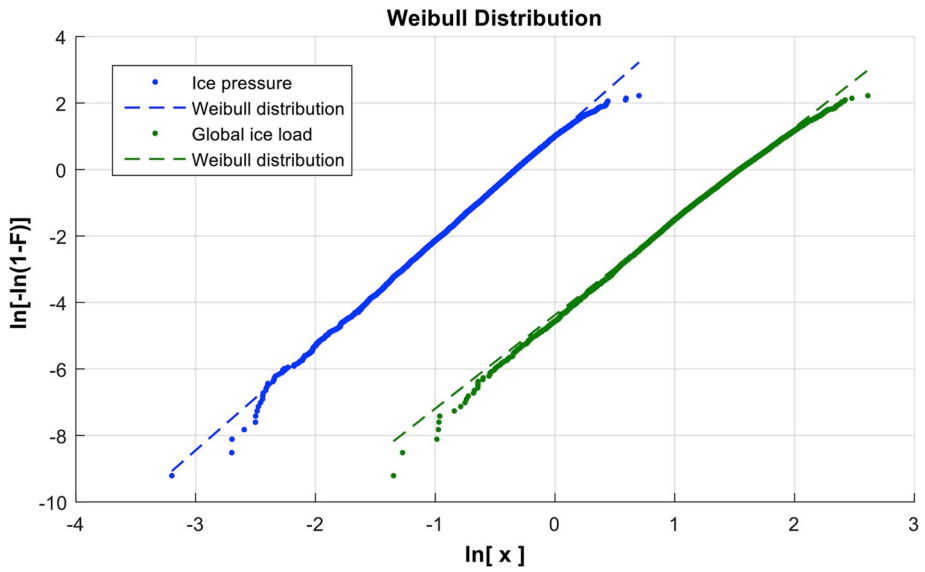

Fig. 23. Example of linear regression for fitting of average ice pressure and global ice forces for vertical structure based on Weibull distribution paper (ρ = 0.0and width = 1.00 m).
(The parameter, x can be ice pressure (in MPa) or global ice force (in MN)).

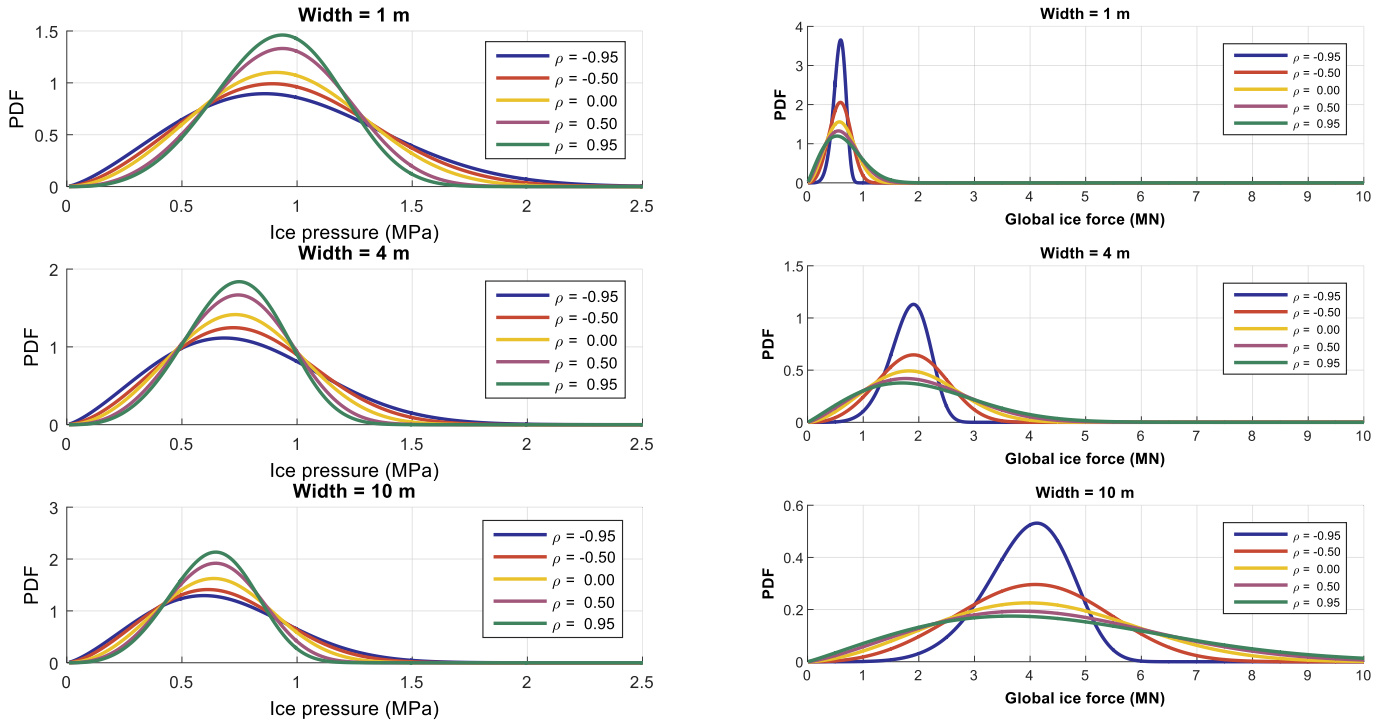

Fig. 24. Relationships between average ice pressure and global ice loads for vertical structures as function of ice thickness and crushing strength for varying structural width values.

downward directions can also be observed in the PDFs as shown in Figs. 30 and 31, respectively. The correlation coefficients between the ice thickness and flexural strength of sea ice demonstrate a significant effect to the shapes of PDF for the global ice loading. The shapes of PDFs are flatter when the values of correlation coefficient in both upward and downward directions increase.

For the slope angle, the results of uncertainty assessment present the significant effects only in the horizontal direction of ice loading. The steeper slopes provide the higher dispersion and higher uncertainty in the global horizontal ice forces as shown in Fig. 32. However, the slope effect is not obviously presented in the vertical ice forces, which can be seen in the shape of PDFs as illustrated in Fig. 33.

Furthermore, the results of uncertainty assessment for sloping structures can be summarized in CDFs as illustrated in Fig. 34.

5. Discussion

Intrinsically, sea ice properties are associated with a high uncertainty level. Due to the corresponding large differences between the maximum and minimum values of the parameters which enter the expressions for calculation of the ice loading, the effect of correlation between the parameters can be expected to be significant (i.e. high-high, high-low or

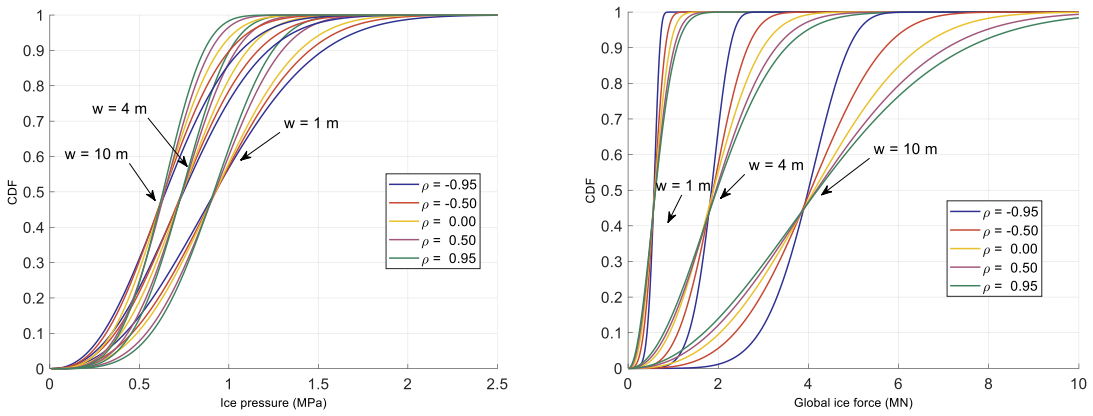

Fig. 25. The Weibull probability density functions of ice pressures per square metre for vertical structures.

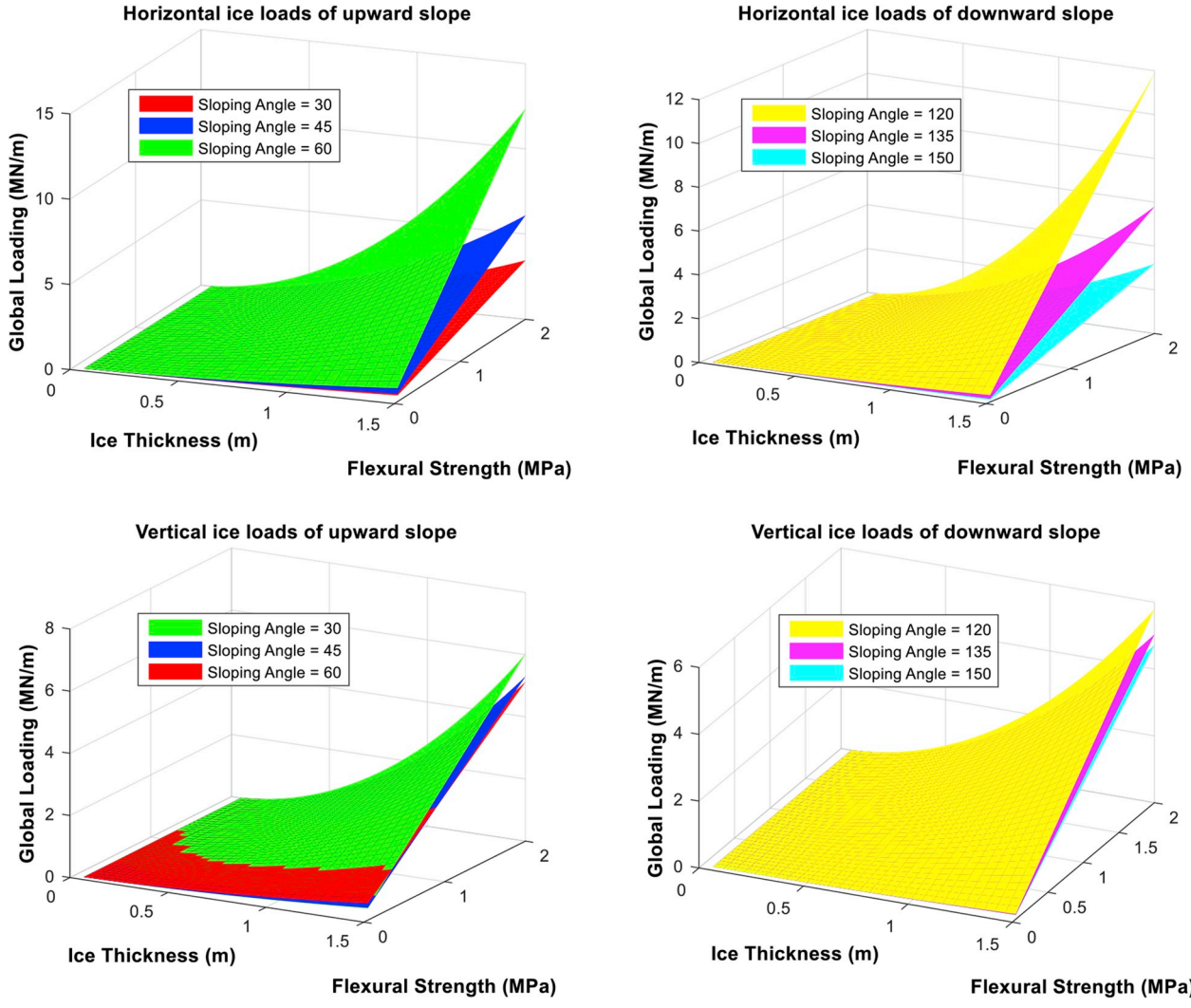

Fig. 26. Relationships of the horizontal and vertical ice loads on sloping structures corresponding to the varying ice thickness, flexural strength and sloping angles.

low-low combinations). This effect is considered in the present study. Furthermore, based on different experimental data sets obtained from field measurements (Figs. 8 and 9), we found that there exists a certain degree of correlation between key design parameters for both vertical and sloping structures. Based on a probabilistic analysis, the effect of correlation between sea ice properties on the computed ice loads can be readily taken into account. This is achieved by utilization of multivariate probability density functions (which include the relevant correlation coefficients as explicit parameters) in combination with Monte Carlo simulation techniques. The corresponding effect on the resulting ice load magnitude, which is calculated based on the formulation in the widely applied ISO standard, can then be quantified. For the analysis, correlation coefficient values in the entire range from the lowest to highest values are considered, (i.e. between −1 and +1 For computational

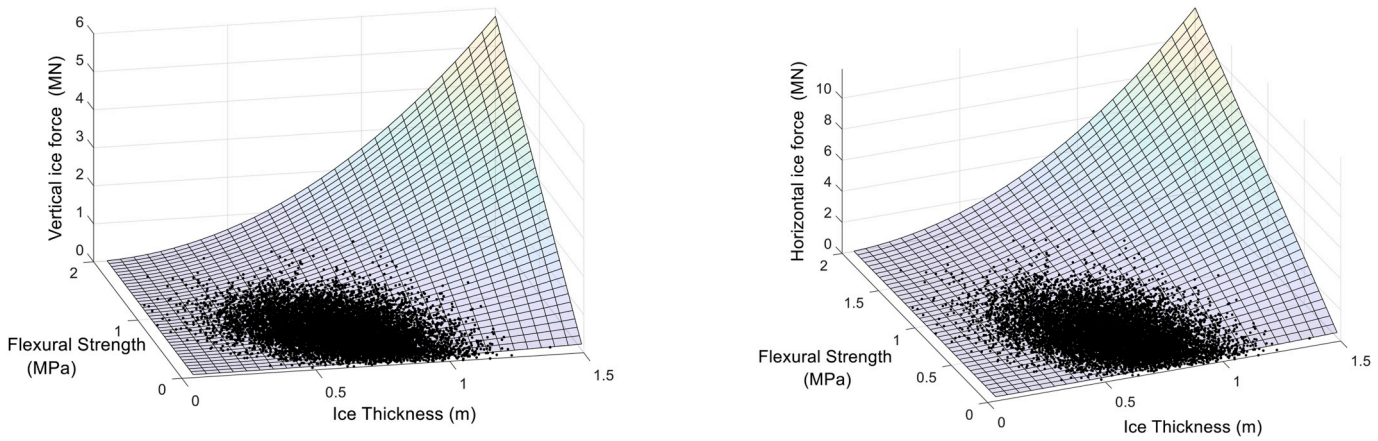

Fig. 27. Samples of the vertical and horizontal ice forces based on an application of the NATAF transformation model for $\rho = -0.5$ and sloping angle = 30 deg. (upward direction).

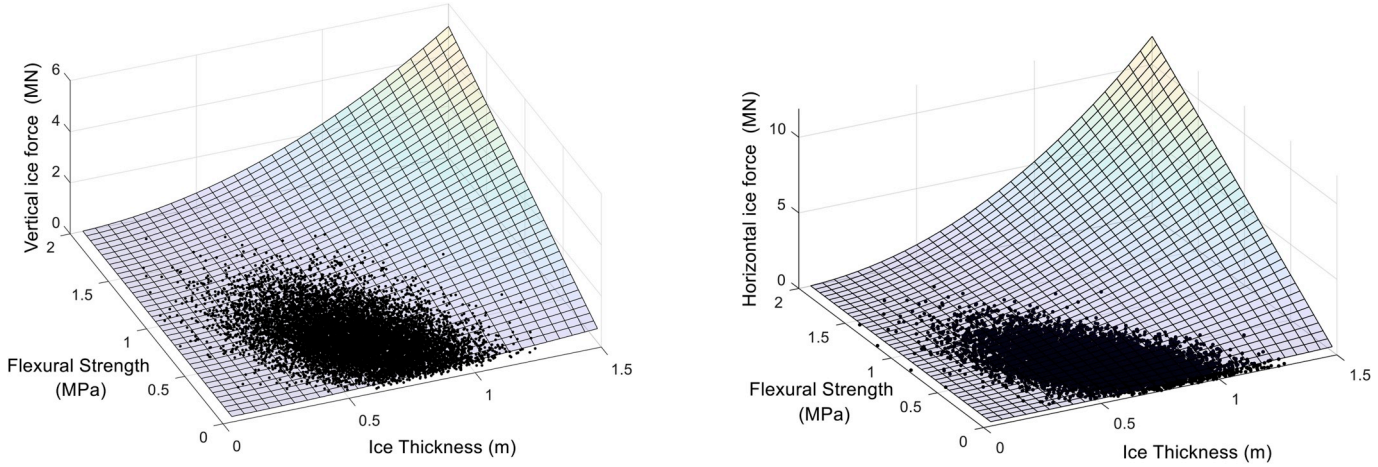

Fig. 28. Samples of the vertical and horizontal ice forces based on an application of the NATAF transformation model for $\rho = -0.5$ and sloping angle = 120 deg. (downward direction).

Table 4
Statistical characteristics of global horizontal and vertical ice forces on sloping structures for different correlation coefficients and different sloping angels in the upward direction.

Angle (deg.)	ρ	Horizontal ice force (MN)				Vertical ice force (MN)			
		Mean	STD	COV%	kurtosis	Mean	STD	COV%	kurtosis
30	−0.9	0.192	0.036	18.75	5.496	0.285	0.054	18.95	5.496
30	−0.5	0.210	0.095	45.24	4.448	0.311	0.141	45.34	4.448
30	0	0.230	0.145	63.04	6.382	0.341	0.215	63.05	6.382
30	0.5	0.250	0.191	76.40	8.895	0.371	0.283	76.28	8.895
30	0.9	0.267	0.223	83.52	8.718	0.395	0.331	83.80	8.718
45	−0.9	0.298	0.056	18.79	5.273	0.259	0.048	18.53	5.273
45	−0.5	0.327	0.157	48.01	5.138	0.284	0.137	48.24	5.138
45	0	0.368	0.249	67.66	6.457	0.320	0.216	67.50	6.457
45	0.5	0.403	0.326	80.89	8.472	0.350	0.283	80.86	8.472
45	0.9	0.434	0.384	88.48	9.463	0.377	0.334	88.59	9.463
60	−0.9	0.560	0.108	19.29	4.832	0.273	0.053	19.41	4.832
60	−0.5	0.628	0.324	51.59	5.715	0.306	0.158	51.63	5.715
60	0	0.697	0.487	69.87	7.394	0.340	0.237	69.71	7.394
60	0.5	0.775	0.650	83.87	9.313	0.378	0.317	83.86	9.313
60	0.9	0.833	0.765	91.84	9.608	0.406	0.373	91.87	9.608

purposes, the correlation coefficient is assigned values in the range from −0.9 to 0.9 in order to avoid numerical problems.

The degree of uncertainty associated with the ice loads is quantified in terms of the coefficient of variation, i.e. the COV. High values of the COV imply high levels of uncertainty. Moreover, the levels of uncertainty can also be observed based on the shape of the PDFs and CDFs, i.e. flatter shape of the PDFs and a smaller slope of the CDFs imply higher levels of uncertainty. Characteristic values of the ice loads to be applied for design purposes can be determined by means of upper fractiles of the corresponding probability distributions, (Ditlevsen and

Table 5
Statistical characteristics of global horizontal and vertical ice forces on sloping structures for different correlation coefficients and different sloping angels in the downward direction.

Angle	ρ	Horizontal ice force (MN)				Vertical ice force (MN)			
		Mean	STD	COV	kurtosis	Mean	STD	COV	kurtosis
120	−0.9	0.438	0.107	24.43	3.746	0.214	0.052	24.43	3.746
120	−0.5	0.501	0.290	57.88	5.747	0.244	0.141	57.88	5.747
120	0	0.582	0.468	80.41	9.031	0.284	0.228	80.41	9.031
120	0.5	0.653	0.600	91.88	8.824	0.318	0.292	91.88	8.824
120	0.9	0.712	0.715	100.42	10.579	0.347	0.349	100.42	10.579
135	−0.9	0.221	0.053	23.98	3.830	0.192	0.046	23.98	3.830
135	−0.5	0.252	0.145	57.54	5.216	0.219	0.126	57.54	5.216
135	0	0.293	0.229	78.16	7.661	0.254	0.199	78.16	7.661
135	0.5	0.326	0.296	90.80	8.482	0.283	0.258	90.80	8.482
135	0.9	0.356	0.356	100.00	10.286	0.310	0.309	100.00	10.286
150	−0.9	0.123	0.029	23.58	3.799	0.182	0.044	23.58	3.799
150	−0.5	0.140	0.080	57.14	5.388	0.207	0.118	57.14	5.388
150	0	0.160	0.124	77.50	7.650	0.238	0.184	77.50	7.650
150	0.5	0.181	0.167	92.27	10.300	0.269	0.247	92.27	10.300
150	0.9	0.198	0.197	99.49	10.570	0.293	0.291	99.49	10.570

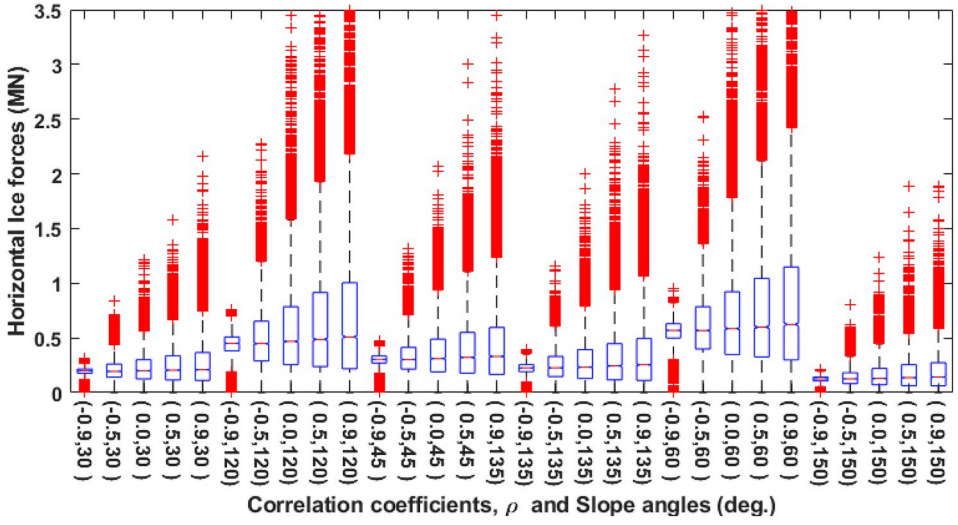

Fig. 29. Box-and-whisker diagram for horizontal ice force on sloping structures with different correlation coefficient and slop angles.

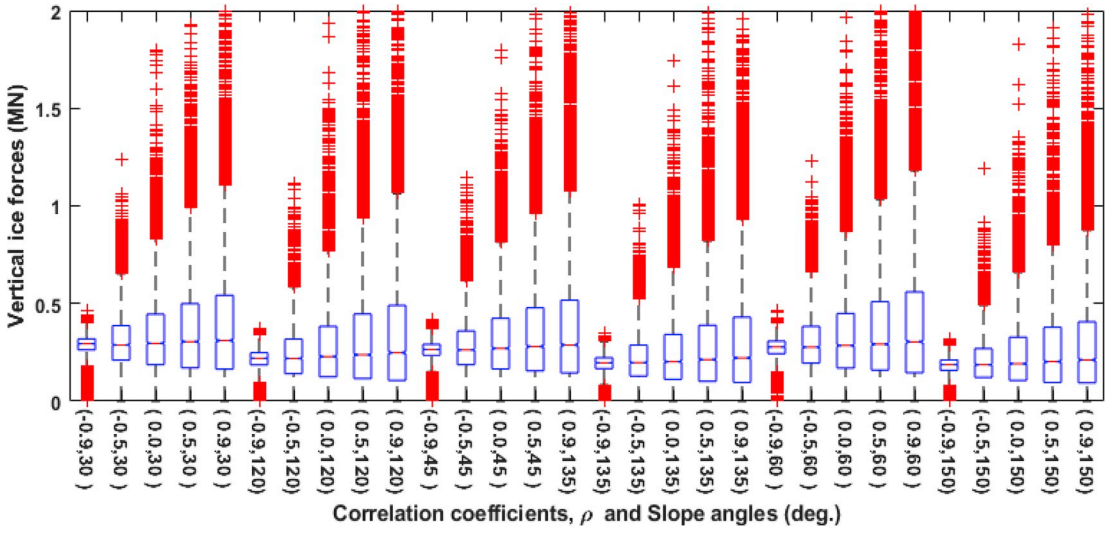

Fig. 30. Box-and-whisker diagram for vertical ice force on sloping structures with different correlation coefficient and slop angles.

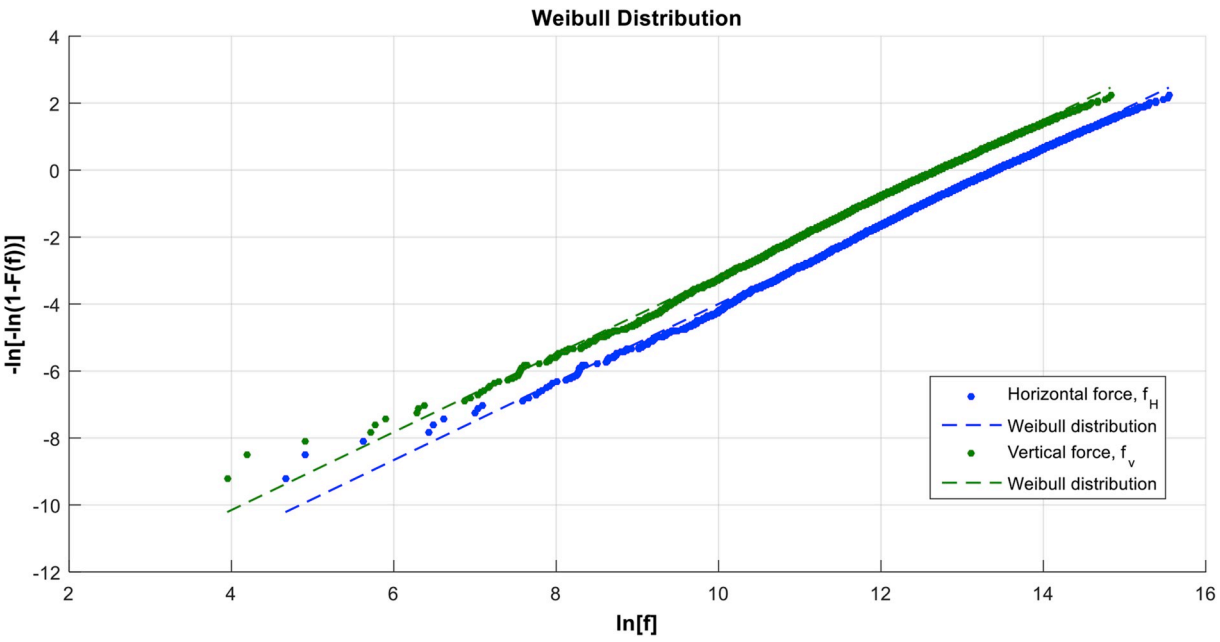

Fig. 31. Example of linear regression for fitting of horizontal and vertical ice forces on sloping structure based on the Weibull probability paper ($\rho = 0.0$and slope angle $= 120$ deg.). The parameter, f represents the global horizontal ice force or the global vertical ice force.

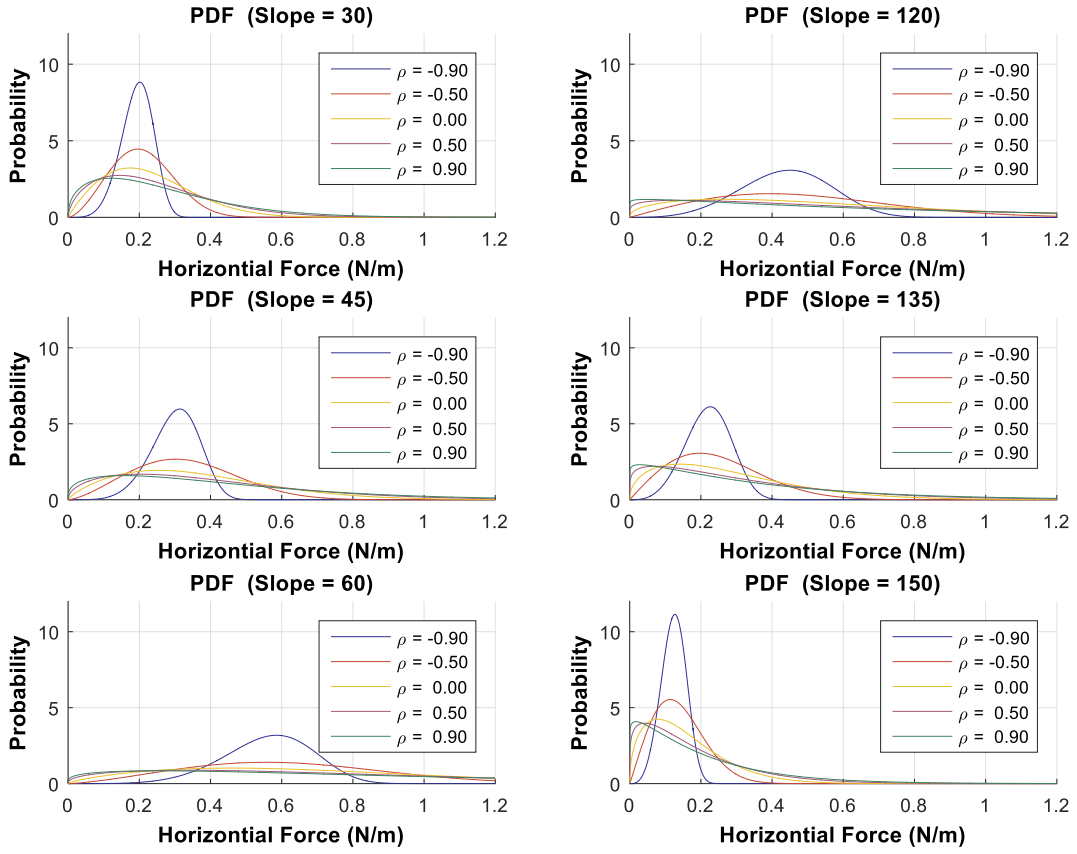

Fig. 32. Weibull probability density functions for horizontal ice forces on sloping structures for different correlation coefficients and sloping angles.

Madsen, 1996). Increasing uncertainty levels imply that the ratio of a given fractile to the mean value will increase accordingly. For design purpose, the characteristic values of the loads (i.e. the fractile values) are subsequently multiplied partial load coefficients in order to ensure an adequate level of structural reliability (Ditlevsen and Madsen, 1996). Typically, characteristic design values for external loads are taken to be the 95% fractile or above. In the present study, the 99% fractile is utilized in order to demonstrate the influence from the degree of correlation between key design parameters on the resulting ice loading for both vertical and sloping structures.

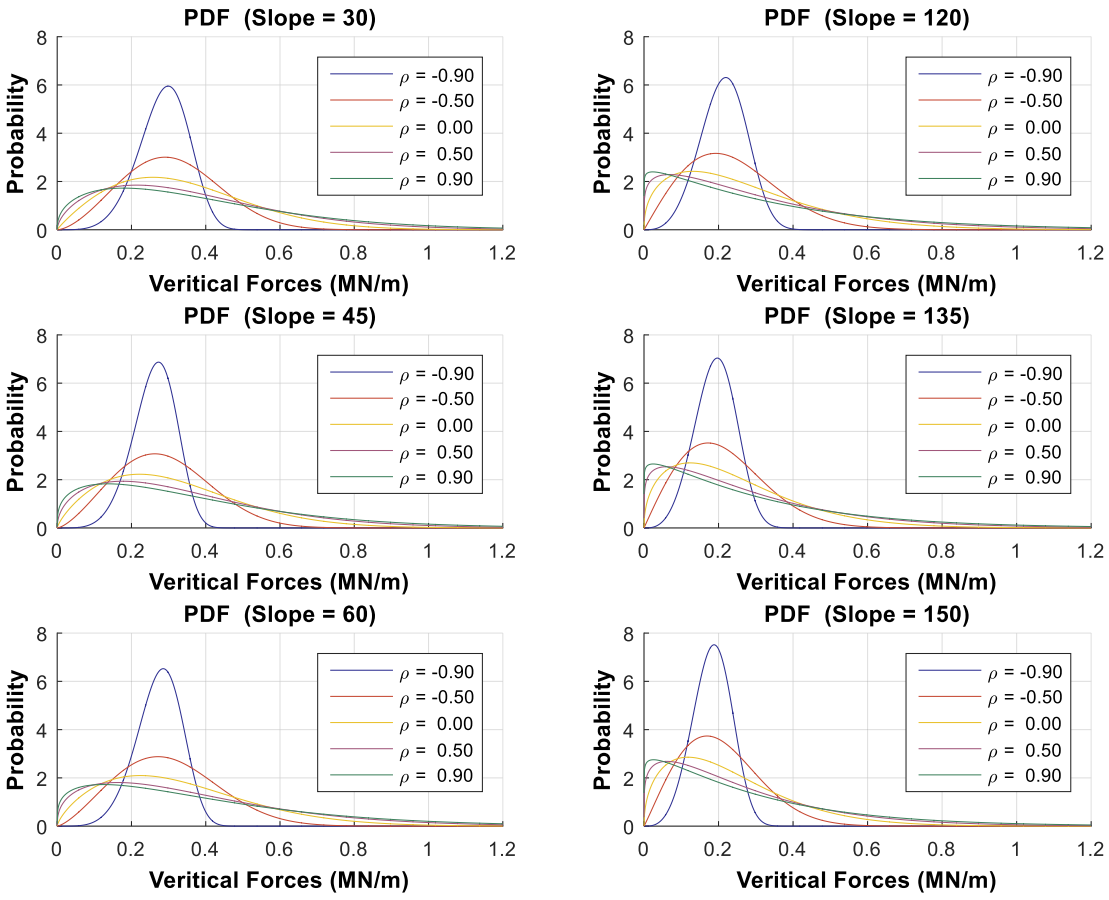

Fig. 33. Weibull probability density functions for vertical ice forces on sloping structures for different correlation coefficients and sloping angles.

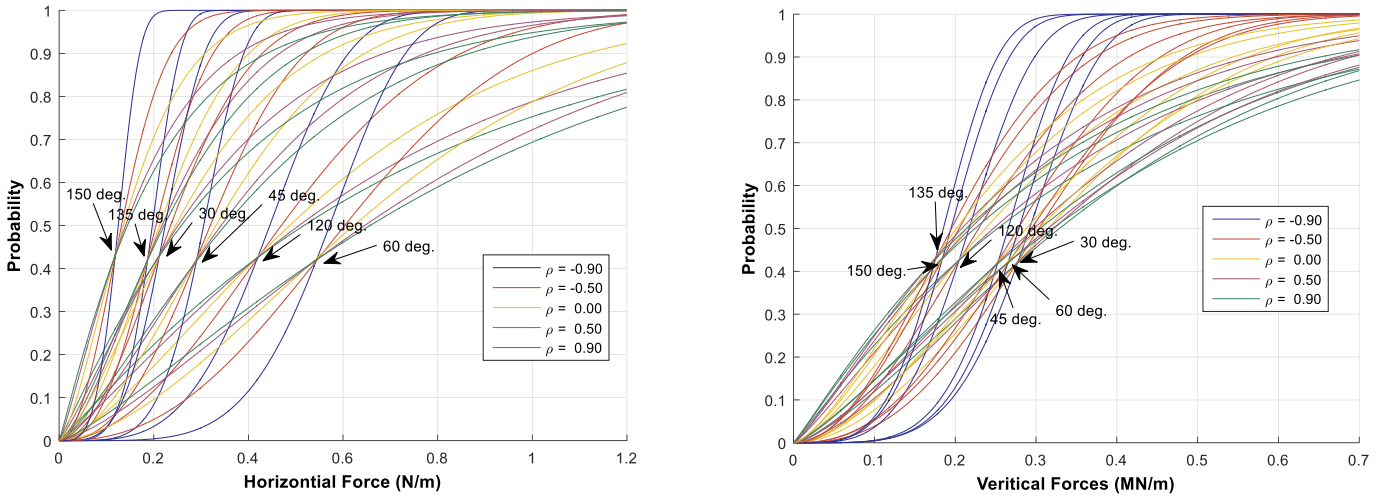

Fig. 34. Weibull cumulative distribution functions of horizontal and vertical ice loads for sloping structures based on different correlation coefficients and sloping angles.

5.1. Vertical structures

For calculation of ice loads acting on vertical structures based on the ISO standard, the ice thickness and ice strength coefficient are key parameters for estimation of the ice pressure and the global ice forces. The correlation coefficients between these quantities can be estimated based on measurements of loads acting on panels, which are attached to the structures. Values of the observed correlation between the ice thickness and the ice strength coefficient from four experiments are −0.574, −0.408, −0.014 and 0.413, respectively. The observed values of the correlation coefficient tends to be in the negative side, which can also be observed from Fig. 8 in section 2.4.

It is found that the effects of changing the correlation coefficient between ice thickness and ice strength coefficient exhibit opposite trends for the ice pressure versus the global ice force. This is clearly observed from the PDFs and CDFs of the ice pressure and global ice force in Figs. 24 and 25. The relevant statistical parameters for calculation of the 99% fractiles of the ice pressure and global ice force are listed in

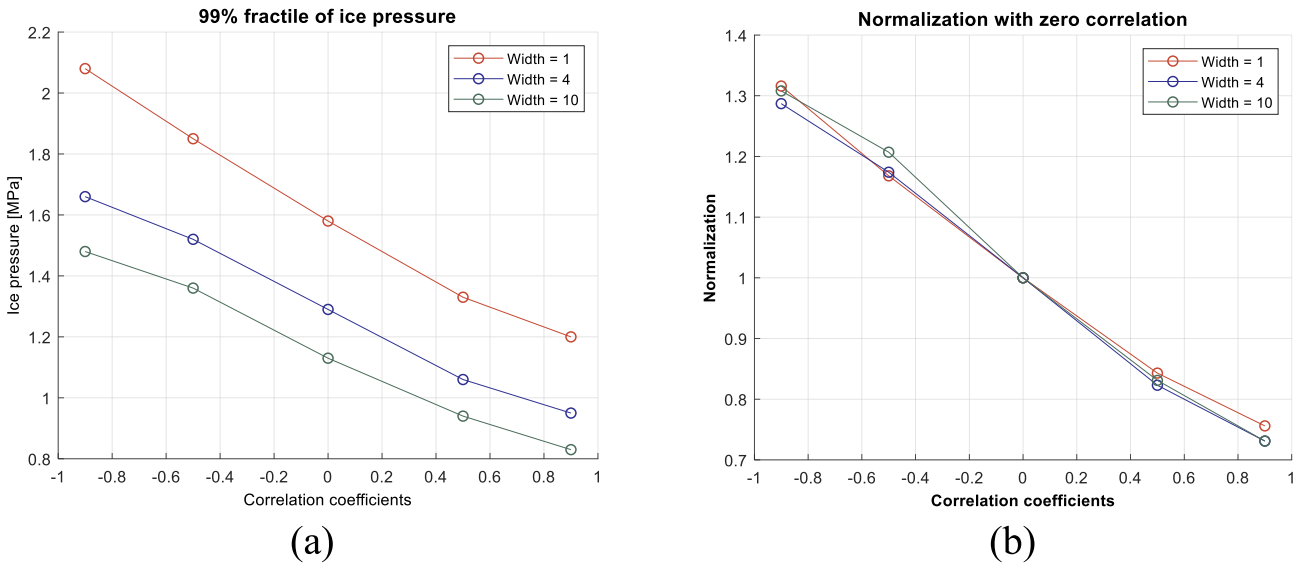

Fig. 35. a) 99% fractile of ice pressure vs. correlation. b) Normalization of the 99% fractile of ice pressure with the value for the zero correlation case (for widths of 1m, 4m and 10m).

Table 3. The effect of varying the correlation coefficient on this fractile for the ice pressure and global ice load is shown in Figs. 35 and 36, respectively. As seen from Fig. 35a, negative values of the correlation coefficient imply higher values of the 99% fractile for the ice pressure. On the contrary, Fig. 36a shows that positive values of correlation coefficient provides higher values of 99% fractile for the global ice force. This can be further demonstrated by normalizing the 99% fractiles with the value corresponding to zero correlation. As can be seen from Fig. 35b, there is a 30% decrease of the ice pressure by going from a value of the correlation coefficient of 0–0.9. For the global horizontal force there is instead and increase of 40% for the same case as seen from Fig. 36b, respectively.

5.2. Sloping structures

For sloping structures, the level ice thickness, rubble pile-up height and the flexural strength are in some cases important parameters to estimate the ice loading (e.g. for thin ice, narrow structures and no snow). In this analysis, the distributions of accumulated rubble pile-up height according to the empirical formulas from data collected at the Kemi-lighthouse and at the Confederation bridge were estimated based on the probability density functions of level ice thickness by using a one-to-one transformation corresponding to a monotonously increasing function. It found that the results for the Confederation bridge provide the highest values, which can be observed from the PDF of the rubble pile-up height in Fig. 16. Therefore, the results for the Confederation bridge are employed in the computation in order to obtain more conservative global forces. Subsequently, the two parameters corresponding to thickness of the level ice and ice flexural strength represent the key parameters in order to estimate the ice loading on sloping structures.

In the present study, the effects of varying correlation between level ice thickness and ice flexural strength is considered. The correlation coefficient between these quantities was estimated based on data obtained from field measurements at different locations and with different weather conditions. The results of these measurements are illustrated by means of joint sets of data points in Fig. 9 in section 2.4. The values of

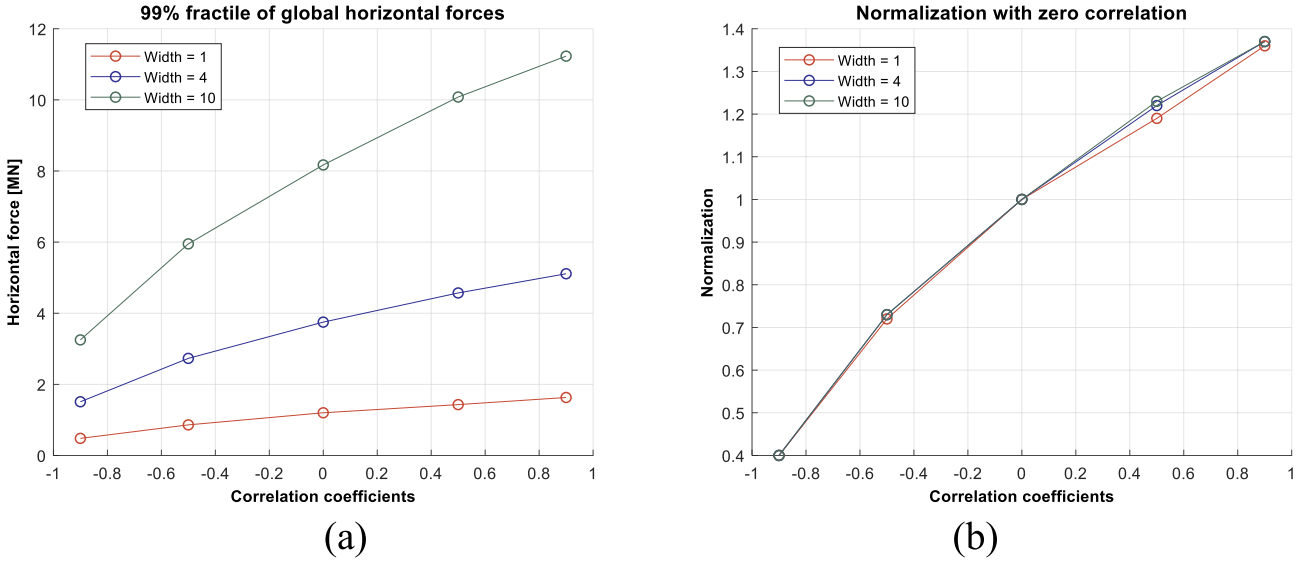

Fig. 36. a) 99% fractile of horizontal ice force vs. correlation. b) Normalization of the 99% fractile of horizontal ice force with the value for the zero correlation case (for widths of 1m, 4m and 10m).

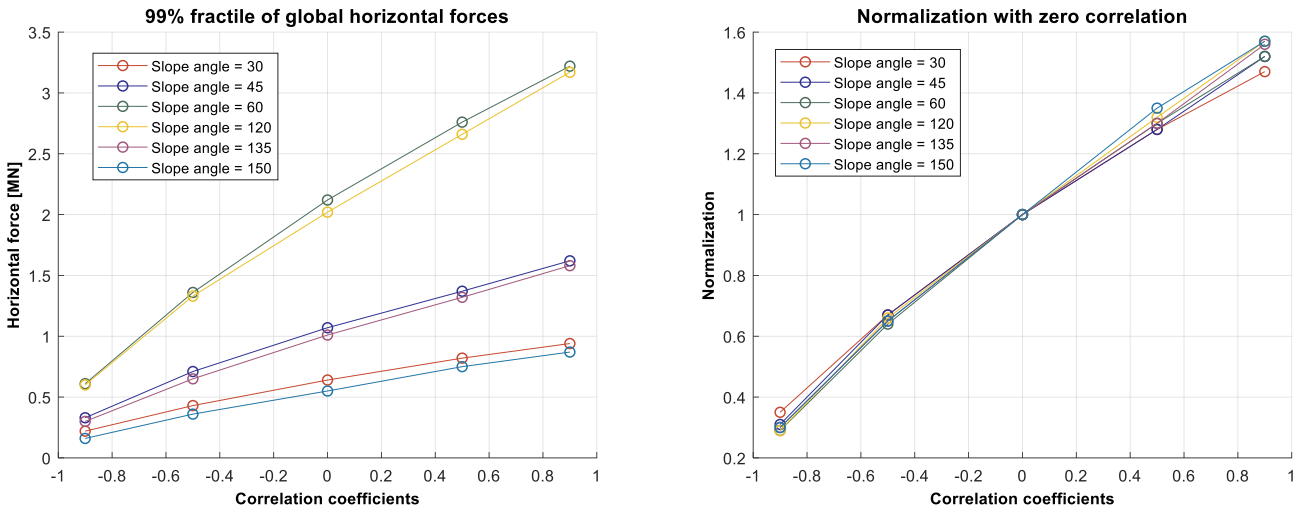

Fig. 37. a) 99% fractile of global horizontal ice force vs. correlation. b) Normalization of 99% fractile of ice pressure with zero correlation case (for slope angles in the range from 30 to 150°).

correlation coefficient which was estimated from each of the data sets are found to be −0.310, −0.322, 0.764 and 0.566, respectively. Merging all the data sets, the correlation coefficients was estimated as 0.66.

The effects of varying the correlation coefficient on the resulting PDFs and CDFs are illustrated by the results in Figs. 32–34. The corresponding values of the COV are listed in Tables 4 and 5 The variation of the value of the 99% fractile resulting from variation of the correlation coefficient is shown in Fig. 37a (horizontal force) and 38b (vertical force) for different values of the sloping angle. The corresponding results obtained by normalizing the 99% fractile of the global horizontal and vertical forces with the values corresponding to zero correlation are shown in Figs. 37b and 38b. It is seen that there is an increase of about 60% when going from a correlation coefficient of zero to 0.9 for both the horizontal and the vertical load components.

The action factors and action combination factors for ISO 19906:2010 to be applied for the ultimate limit state (ULS) and the abnormal limit state(ALS) in relation to environmental actions including ice loads are about 1.35 and 1.10 for respectively the highest and the intermediate exposure levels. In the present study, the effects of correlation between key design parameters with respect to the calculated ice loads are quantified by comparison with the case of zero correlation. The normalized values of the global ice loads increase approximately 40% and 60% for a correlation coefficient of 0.9 (as compared to the case with zero correlation) for the case of vertical and sloping structures, respectively. However, the correlation between the relevant design parameters will usually have a value between 0 and 0.9 (and it can also be negative). Therefore, more extensive studies of the proper correlation to be applied for calculation of design ice loads than those reported in the literature should be performed. This could result in "load parameter combination factors" to be applied for selection of joint parameter values to be applied for design purposes.

6. Conclusions

A probabilistic assessment of loads due to ice-structure interaction based on the formula in the ISO standard has been performed by means of Monte-Carlo simulation techniques. Two types of structures are analysed, i.e. with vertical and sloping configurations, respectively. The correlation coefficient between the ice strength coefficient and the ice thickness as well as the correlation coefficient between the flexural strength and the ice thickness were estimated, and the corresponding effects on the uncertainties associated with the ice loads were investigated for varying values of the correlation coefficients. The degree of uncertainty associated with the ice loads was quantified in terms of COV

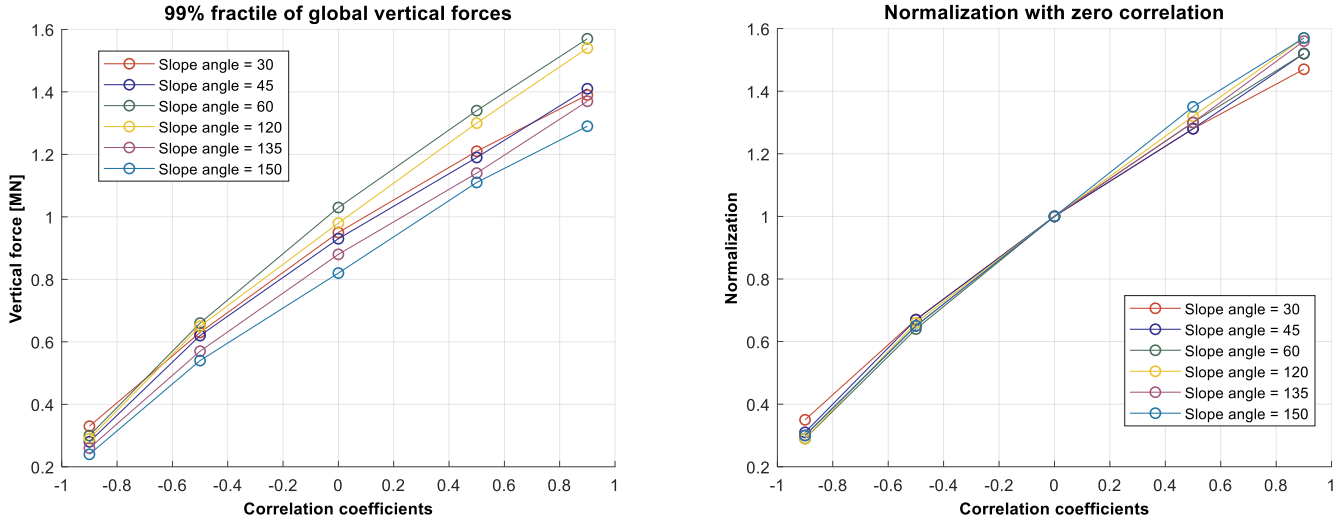

Fig. 38. a) 99% fractile of global vertical ice force vs. correlation. b) Normalization of 99% fractile of ice pressure with zero correlation case (for slope angles in the range from 30 to 150°).

values, i.e. higher values of the COV imply higher levels of uncertainty. For practical design, the fractile values are usually employed in combination with the partial load factors in order to ensure adequate structural reliability levels.

Our analysis shows that both the global ice force and its associated uncertainty increased for high values of the correlation coefficients as compared to the case with zero correlation.

- For vertical structures, the mean values, the standard deviations, the COVs and the 99% fractile of the global forces increased by approximately 10%, 40%, 30% and 40%, respectively, when going from a correlation coefficient of 0–0.9.
- For sloping structures, the mean value, the standard deviation, the COV and the 99% fractile of the global horizontal and vertical forces increase by approximately 20%, 60%, 35% and 60%, respectively, when going from a correlation coefficient of 0–0.9.
- For sloping structures, higher values of the sloping angles imply higher values of the standard deviation. This applies accordingly also to the COV and the fractile values associated with the global forces.
- Changing the slope angle will have a stronger influence on the mean values, the standard deviations, the COVs and the fractile values for the global forces in the horizontal direction as compared to the global forces in the vertical direction.

Quantification of the uncertainty associated with the environmental ice loading on offshore structures is required in order to enhance the accuracy associated with choice of partial load factors for structural design purposes. This applies to the limit state design. This also implies an increase of the reliability level of the structures during their operation due to more accurate information. Accordingly, the types of probability density functions and the values of the relevant correlation coefficients for a proper statistical characterization of sea ice loading should be selected with care. This is in order to perform a precise assessment of the structural reliability level associated with design of offshore structures in the regions being considered.

It is emphasized that model uncertainties associated with the applied load models have not been included as part of the present study. In order to assess the implied safety level associated with application of the given design formulas and corresponding partial coefficients such model uncertainty factors are also required and will be an important extension of the present work.

CRediT authorship contribution statement

Chana Sinsabvarodom: Formal analysis, Writing - original draft. **Wei Chai:** Formal analysis, Writing - original draft. **Bernt J. Leira:** Formal analysis, Writing - original draft. **Knut V. Høyland:** Formal analysis, Writing - original draft. **Arvid Naess:** Formal analysis.

Acknowledgments

This work is supported by NTNU Oceans Pilot project Risk, Reliability and Ice Data in arctic marine environment. The authors wish to thank Ilija Samardžija for valuable discussions in connection with modelling of ice loads.

References

Ayubian, S., Alawneh, S., Thijssen, J., 2016. GPU-based monte-carlo simulation for a sea ice load application. In: Proceedings of the Summer Computer Simulation Conference. Society for Computer Simulation International, p. 22.

Bekker, A.T., Sabodash, O.A., Kochev, A.Y., 2011a. Analysis of ice loads on offshore structures for okhotsk sea oil and gas fields. In: ASME 2011 30th International Conference on Ocean, Offshore and Arctic Engineering. American Society of Mechanical Engineers, pp. 439–448.

Bekker, A.T., Sabodash, O.A., Kochev, A.Y., 2011b. Analysis of ice loads on offshore structures for okhotsk sea Oil&Gas fields. Omae2011: Proceedings of the Asme 30th International Conference on Ocean, Offshore and Arctic Engineering 2, 439–448.

Brown, T.G., Määttänen, M., 2009. Comparison of Kemi-I and Confederation Bridge cone ice load measurement results. Cold Reg. Sci. Technol. 55 (1), 3–13.

Bruun, P.K., Gudmestad, O.T., 2006. A comparison of ice loads from level ice and ice ridges on sloping offshore structures calculated in accordance with different international and national standards. In: 25th International Conference on Offshore Mechanics and Arctic Engineering. American Society of Mechanical Engineers, pp. 655–665.

Croasdale, K., Cammaert, A., 1994. An improved method for the calculation of ice loads on sloping structures in first-year ice. Hydrotech. Constr. 28 (3), 174–179.

Ditlevsen, O., Madsen, H.O., 1996. Structural Reliability Methods. Wiley, New York.

Ervik, Å., 2013. Experimental and Numerical Investigations of Cantilever Beam Tests in Floating Ice Covers. NTNU master thesis.

Frederking, R., 2012. Review of Standards for Ice Forces on Port Structures, Cold Regions Engineering 2012: Sustainable Infrastructure Development in a Changing Cold Environment, pp. 725–734.

Hisette, Q., Alekseev, A., Seidel, J., 2017. Discrete element simulation of ship breaking through ice ridges. In: The 27th International Ocean and Polar Engineering Conference. International Society of Offshore and Polar Engineers.

ISO, B., 2010. 19906: 2010. Petroleum and Natural Gas Industries–Arctic Offshore Structures.

Jordaan, I.J., 2001. Mechanics of ice–structure interaction. Eng. Fract. Mech. 68 (17–18), 1923–1960.

Kärnä, T., Masterson, D., 2011. Data for crushing formula. In: Proceedings of the International Conference on Port and Ocean Engineering under Arctic Conditions.

Kärnä, T., Yan, Q., 2006. Analysis of the Size Effect in Ice Crushing-Edition.

Langhorne, P.J., Haskell, T.G., 2004. The flexural strength of partially refrozen cracks in sea ice. In: The Fourteenth International Offshore and Polar Engineering Conference. International Society of Offshore and Polar Engineers.

Lau, M., Lawrence, K.P., Rothenburg, L., 2011. Discrete element analysis of ice loads on ships and structures. Ships Offshore Struct. 6 (3), 211–221.

Leira, B.J., Chai, W., Sinsabvarodom, C., 2019. On correlation and underlying physics. In: Proceedings of the 29th Ecropean Safety and Reliability Conference.

Li, H., Bjerkås, M., V Høyland, K., Nord, T., 2016. Panel loads and weather conditions at Norströmsgrund lighthouse. In: 23rd IAHR International Symposium on Ice Ann Arbor, Michigan USA.

Liu, P.-L., Der Kiureghian, A., 1986. Multivariate distribution models with prescribed marginals and covariances. Probabilistic Eng. Mech. 1 (2), 105–112.

Paquette, E., Brown, T.G., 2017. Ice crushing forces on offshore structures: global effective pressures and the ISO 19906 design equation. Cold Reg. Sci. Technol. 142, 55–68.

Pfaffling, A., Haas, C., Reid, J.E., 2007. Direct helicopter EM—sea-ice thickness inversion assessed with synthetic and field data. Geophysics 72 (4), F127–F137.

Ranta, J., Polojärvi, A., Tuhkuri, J., 2018. Ice loads on inclined marine structures-Virtual experiments on ice failure process evolution. Mar. Struct. 57, 72–86.

Ronkainen, I., Lehtiranta, J., Lensu, M., Rinne, E., Haapala, J., Haas, C., 2018. Interannual sea ice thickness variability in the Bay of Bothnia. Cryosphere 12, 3459–3476.

Saeki, H., Ono, T., Nakazawa, N., Sakai, M., Tanaka, S., 1986. The coefficient of friction between sea ice and various materials used in offshore structures. J. Energy Resour. Technol. 108 (1), 65–71.

SHMI, 2019. Öppna Data, Meteorologiska Observationer [Online]. http://opendata-download-metobs.smhi.se/explore/?parameter=2#. (Accessed June 2019).

Strub-Klein, L., 2017. A statistical analysis of first-year level ice uniaxial compressive strength in the svalbard area. J. Offshore Mech. Arct. Eng. 139 (1), 011503.

Thijssen, J., Fuglem, M., Richard, M., King, T., 2014. Implementation of ISO 19906 for probabilistic assessment of global sea ice loads on offshore structures encountering first-year sea ice. In: Oceans-St. John's, 2014. IEEE, pp. 1–8.

Timco, G.W., O.'Brien, S., 1994. Flexural strength equation for sea ice. Cold Reg. Sci. Technol. 22 (3), 285–298.

Tuhkuri, J., Polojärvi, A., 2018. A review of discrete element simulation of ice–structure interaction. Philos. Trans. R. Soc. A Math. Phys. Eng. Sci. 376 (2129), 20170335.

Wang, B., Basu, R., Jha, A., Winterstein, S., 2011. Reliability analysis of ice loads on Arctic offshore structures. In: Proceedings of the International Conference on Port and Ocean Engineering under Arctic Conditions.

Zubov, N., 1943. Arctic Ice. Izdatel'stvo Glavsevmorputi, Moscow, p. 360.

Zvyagin, P., 2015. A method for the probabilistic modelling of ice pressure. Cold Reg. Sci. Technol. 118, 112–119.